การพัฒนาวัสดุต้านเชื้อแบคทีเรียชนิดใหม่จากเซลลูโลสดัดแปร

นางสาวอภิรดี โอภิธากรณ์

วิทยานิพนธ์นี้เป็นส่วนหนึ่งของการศึกษาตามหลักสูตรปริญญาวิทยาศาสตรมหาบัณฑิต
สาขาวิชาเคมี ภาควิชาเคมี
คณะวิทยาศาสตร์ จุฬาลงกรณ์มหาวิทยาลัย
ปีการศึกษา 2558

DEVELOPMENT OF NOVEL ANTIBACTERIAL MATERIALS BASED ON MODIFIED CELLULOSE

Miss Apiradee Opitakorn

A Thesis Submitted in Partial Fulfillment of the Requirements

for the Degree of Master of Science Program in Chemistry

Department of Chemistry

Faculty of Science

Chulalongkorn University

Academic Year 2015

Thesis Title	DEVELOPMENT OF NOVEL ANTIBACTERIAL MATERIALS BASED ON MODIFIED CELLULOSE
By	Miss Apiradee Opitakorn
Field of Study	Chemistry
Thesis Advisor	Thanit Praneenararat, Ph.D.

Accepted by the Faculty of Science, Chulalongkorn University in Partial Fulfillment of the Requirements for the Master's Degree

.....Dean of the Faculty of Science
(Associate Professor Polkit Sangvanich, Ph.D.)

THESIS COMMITTEE

.....Chairman
(Associate Professor Vudhichai Parasuk, Ph.D.)

.....Thesis Advisor
(Thanit Praneenararat, Ph.D.)

.....Examiner
(Panuwat Padungros, Ph.D.)

.....External Examiner
(Assistant Professor Chutima Jiarpinitnun, Ph.D.)

อภิรดี โอภิธากรณ์ : การพัฒนาวัสดุต้านเชื้อแบคทีเรียชนิดใหม่จากเซลลูโลสดัดแปร (DEVELOPMENT OF NOVEL ANTIBACTERIAL MATERIALS BASED ON MODIFIED CELLULOSE) อ.ที่ปรึกษาวิทยานิพนธ์หลัก: ดร.ธนิษฐ์ ปราณีนรารัตน์, หน้า.

การยับยั้งการเจริญเติบโตของแบคทีเรียที่ก่อโรคมีความสำคัญในการประยุกต์ใช้ด้านต่างๆ มากมาย เช่น ในระบบการขนส่งยา, อุตสาหกรรมสิ่งทอ, อุตสาหกรรมเครื่องมือ-อุปกรณ์ทางการแพทย์ และ อุตสาหกรรมอาหาร ในปัจจุบันวัสดุสิ่งทอที่มีฤทธิ์ฆ่าแบคทีเรียเมื่อมีการสัมผัส (contact-based bactericidal textiles) มักทำโดยการดัดแปรด้วยเพปไทด์ต้านแบคทีเรียที่ถูกสังเคราะห์ขึ้น ซึ่งในงานวิจัยนี้ได้สังเคราะห์เพปไทด์สายสั้น (RIGRR) ลงบนพื้นผิวคอตตอนด้วยพันธะโควาเลนต์ แล้วดัดแปรด้วยการต่อกรดไขมันชนิดอิ่มตัวที่สายโซ่ยาวแตกต่างกัน (C4, C6, C10, C12, C16, และ C18) เพื่อเพิ่มคุณสมบัติความไม่ชอบน้ำ (hydrophobicity) ด้วยวิธี SPOT และ Fmoc chemistry จากนั้นศึกษาลักษณะจำเพาะโดยการวิเคราะห์ด้วยเทคนิคยูวี-วิสิเบิลสเปกโทรสโกปี (UV-Visible spectroscopy), กล้องจุลทรรศน์อิเลคตรอนแบบส่องกราด (Scanning Electron Microscopy, SEM) และเทคนิคมัลดิ-ทอฟแมสสเปกโทรเมตรี (MALDI-TOF Mass spectrometry) สำหรับการทดสอบความสามารถในการยับยั้งเชื้อแบคทีเรียแกรมบวก (*Staphylococcus aureus*-ATTC 6538P) และ แบคทีเรียแกรมลบ (*Escherichia coli*-ATCC 8739 และ *Pseudomonas aeruginosa*-ATTC 9027) ด้วยวิธีการตรวจนับปริมาณโคโลนี (colony counting method, JIS L 1902) พบว่า พื้นผิวคอตตอนดัดแปรดังกล่าวนั้นสามารถฆ่าเชื้อแบคทีเรียแกรมลบได้ดีกว่าแบคทีเรียแกรมบวก นอกจากนี้ได้ศึกษาความเข้ากันได้ทางชีวภาพ (biocompatibility) พบว่าพื้นผิวดัดแปรไม่เป็นพิษต่อเซลล์กล้ามเนื้อในหนู (mouse fibroblasts L929 cell)

ภาควิชา เคมี ลายมือชื่อนิสิต .....

สาขาวิชา เคมี ลายมือชื่อ อ.ที่ปรึกษาหลัก .....

ปีการศึกษา 2558

5672136523 : MAJOR CHEMISTRY

KEYWORDS: ANTIBACTERIAL / AMP / CELLULOSE / COTTON FABRIC

APIRADEE OPITAKORN: DEVELOPMENT OF NOVEL ANTIBACTERIAL MATERIALS BASED ON MODIFIED CELLULOSE. ADVISOR: THANIT PRANEENARARAT, Ph.D., pp.

The inhibition of pathogenic bacterial growth is essential for many practical applications such as drug delivery systems, textiles, medical devices and food industries. The contact-based bactericidal textiles are generally made of conjugated synthetic antimicrobial peptides. In this research, contact-active antimicrobial surfaces were synthesized by introducing short peptides (RIGRR) onto the cotton surfaces through covalent conjugation. Further modifications were performed with the attachment of aliphatic acids with different lengths (C4, C6, C10, C12, C16, and C18) to increase the hydrophobicity via the SPOT method and standard Fmoc chemistry. The peptide-immobilized cotton fabrics were further characterized by UV-Visible spectrophotometry, Scanning Electron Microscopy (SEM) and MALDI-TOF Mass spectrometry. The functionalized cotton fabrics were evaluated for their antibacterial activity by colony counting method (JIS L 1902) against Gram-positive bacterium (*Staphylococcus aureus*-ATTC 6538P), and Gram-negative bacteria (*Escherichia coli*-ATCC 8739, and *Pseudomonas aeruginosa*-ATTC 9027). The results showed that the short peptide-immobilized cotton fabrics exhibited higher antibacterial activity in Gram-negative bacteria. Moreover, evaluation of the biocompatibility of the short peptide-immobilized cotton fabrics indicated that the materials were non-toxic to mouse fibroblasts (L929) cell.

Department: Chemistry Student's Signature .....

Field of Study: Chemistry Advisor's Signature .....

Academic Year: 2015

ACKNOWLEDGEMENTS

I wish to sincerely thank and express my deepest gratitude to Dr. Thanit Praneenararat of the department of chemistry and Assistant Professor Dr. Rungaroon Waditee-Sirisattha of the department of microbiology, for their advice and suggestion, assistance, motivation, immense knowledge for research, and personal friendship throughout the course of my research. Besides, I would like to thank the rest of my thesis committee: Associate Professor Vudhichai Parasuk, Dr. Panuwat Padungros, and Assistant Professor Dr. Chutima Jiarpinitnun for their valuable constructive comments and suggestions.

This thesis would not be successful without kindness and helps from many people. Firstly, I would like to thank Mr. Nuttapon Jirakittiwut, Miss Monrawat Rauytanapanit, and the member of TP lab. In addition, Gratitude is also expressed to Miss Duangjai Sittipol, Miss Warangkana Sopun, Miss Pairpilin Charuchinda, and the member of the RWS lab of the department of microbiology for their useful advice about antibacterial testing, kindness, and strong moral support. I would like to thank Miss Songchan Puthong for her guidance in biocompatibility assays.

This work was supported by the Ratchadaphiseksomphot Endowment Fund of Chulalongkorn University (RES560530078-AM).

Finally, the author also would like to express my heartfelt gratitude toward my parents, my aunt, my family members and Mr.Parinut Somnuk for their love, understanding, encouragement, and financial support throughout my life.

CONTENTS

Page

Page

Page

Page

LIST OF TABLES

Page

LIST OF FIGURES

Page

LIST OF SCHEMES

Page

LIST OF ABBREVIATIONS AND SYMBOLS

%	percent
Å	angstrom
℃	degree celcious
µL	microliter
µM	micromolar
AMPs	antimicrobial peptides
ATTC	american type culture collection
calcd	calculated
CCA	α-cyano-4-hydroxy cinnamic acid
DBU	1,8-diazabicyclo[5.4.0]undec-7-ene
DIC	*N,N'*-diisopropylcarbodiimide
DMF	*N,N'*-dimethylformamide
E. coli	Escherichia coli
EtOH	ethanol
Fmoc	9-fluorenylmethoxycarbonyl
g	gram
HOBt	1-hydroxybenzotriazole hydrate
JIS	Japanese Industrial Standard
MALDI-TOF	matrix-assisted laser desorption/ionization-time of flight
MeOH	methanol
mg	milligram
min	minute(s)
mmol	millimole
mL	milliliter
mM	millimolar
MS	mass spectrometry
m/z	mass to charge ratio

NaOH	sodium hydroxide
NB	Nutrient broth
nm	nanometer
NSS	normal saline solution
OD_{xxx}	optical density at xxx nm
P. aeruginosa	*Pseudomonas aeruginosa*
Pbf	pentamethyl-2,3-dihydrobenzofuran-5-sulfonyl
rpm	revolutions per minute
S. aureus	*Staphylococcus aureus*
tBu	tert-butyl
TFA	trifluoroacetic acid
TIPS	triisopropylsilane
TsCl	*p*-toluenesulfonyl chloride

CHAPTER I
INTRODUCTION

1.1 Bacterial infection

Bacterial attachment on surface can cause the contamination in medical devices, food, textile industries, which lead to many diseases in humans. For medical devices, biofilm formation on medical implants can cause various infections, resulting in serious illness and death [1]. For food industries, harmful microbes may enter the manufacturing process. Bacterial contamination in food processing is the leading cause of food poisoning. In addition, bacterial adherence and growth on textiles affect human health through direct contact with skin. In addition, the antibiotic resistance has emerged, emphasizing the shortcomings in antibiotic development. These problems were partially overcome by the development of antibacterial agents and materials that can prevent bacterial attachment and proliferation. To date, several antimicrobial materials were designed to damage bacterial membrane [2].

1.1.1 Bacterial membrane components

Two major types of bacteria can be differentiated by peptidoglycan layer formations. The difference of these membrane components can be identified using a staining process called a Gram stain. Gram-positive bacteria composed of a thick homogeneous peptidoglycan layer (20-80 nm), consisting of linear polysaccharide chains interlaced with peptide chains to form a three-dimensional rigid structure. In contrast, the Gram-negative bacteria surface is quite complex due to the thin layer (7-8 nm) of the outer membrane, which consists of lipopolysaccharides, followed by a thin layer (2-7 nm) of peptidoglycan. Interestingly, both Gram-negative and Gram-positive bacteria surfaces possess an overall negative charge, due to the presence of teichoic acids and lipoteichoic acids in Gram-positive bacteria, and lipopolysaccharides (LPS) in Gram-negative bacteria (**Figure 1.1**). Bacterial membranes usually differ from the eukaryotic membrane in lacking sterols such as cholesterol [3].

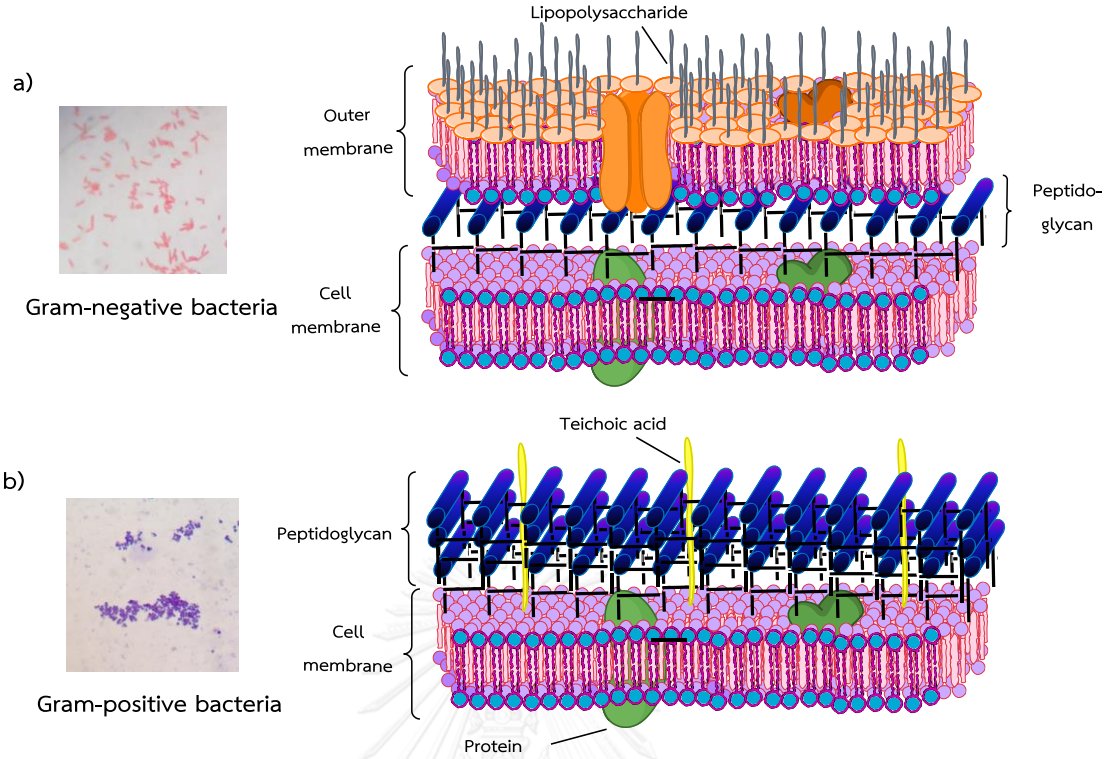

Figure 1.1 Bacterial surfaces of a) Gram-negative bacteria and b) Gram-positive bacteria.

1.1.2 Gram-positive bacteria

Staphylococcus aureus (*S. aureus*) is a Gram-positive coccal bacterium, which is stained purple with crystal violet (**Figure 1.2**). It can infect all tissues of the body and can cause several human diseases such as food poisoning, hospital-acquired infections and skin infections [4].

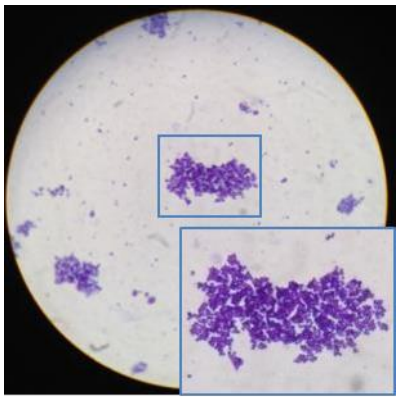

Figure 1.2 Microscopic views of *Staphylococcus aureus*.

1.1.3 Gram-negative bacteria

Escherichia coli (*E. coli*) and *Pseudomonas aeruginosa* (*P. aeruginosa*) are Gram-negative bacteria with rod shape (**Figure 1.3**). These bacteria are stained pink with safranin dye. *E. coli* is commonly found in the lower intestine of warm-blooded organisms. Most strains of *E. coli* are harmless, but some strains can cause food poisoning. *Pseudomonas aeruginosa* is an opportunistic human pathogen. It can cause pneumonia and other infections in several systems such as urinary tract, gastrointestinal, and skin [5].

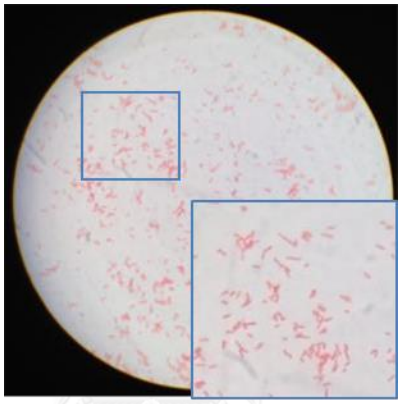

Figure 1.3 Microscopic views of *Escherichia coli*.

1.2 Development of antibacterial surfaces

In recent years, increasing attention has been focused on creating modified surfaces for medical applications. In general, antibacterial surfaces can be divided into two main categories; bactericidal surfaces which directly kill target cells and bacteria-resistant surfaces which prevent bacterial adhesion without killing the target cell [6], [7].

1.2.1 Bactericidal surfaces

The design procedures of bactericidal surfaces can be divided into two categories, namely contact-based bactericidal surfaces and release-based bactericidal surfaces (**Figure 1.4**).

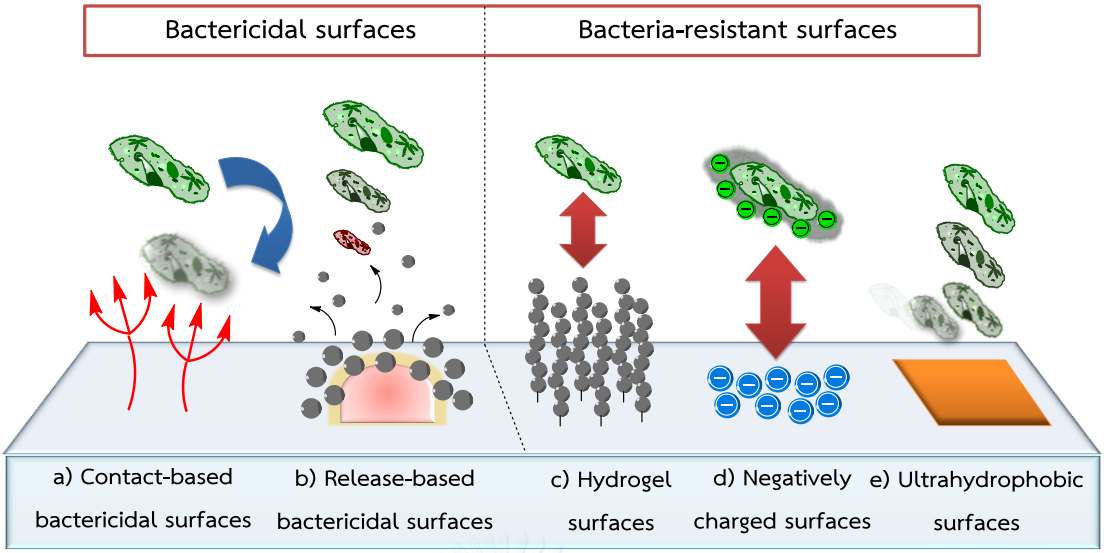

Figure 1.4 General principles of antimicrobial surfaces

1.2.1.1 Contact-based bactericidal surfaces

Contact-based bactericidal surfaces are surfaces that are coated or immobilized with active compounds through covalent conjugation resulting in permanent attachment of active molecules. Such surfaces can be obtained in various ways, including the modification of surfaces using quaternary ammonium compounds (QACs) [8], chitosan and antimicrobial peptides (AMPs) (**Figure 1.4a**).

1.2.1.2 Release-based bactericidal surfaces

Release-based bactericidal surfaces are surfaces that are incorporated with active biocides. The biocides are slowly released into the environment and kill bacteria. The most widely used biocide is silver nanoparticles (AgNPs) [9]. AgNPs is release of Ag^{+}, these ions can bind to the bacterial membrane and cause cell lysis [10] (**Figure 1.4b**).

1.2.2 Bacteria-resistant surfaces

Bacteria-resistant surfaces can prevent bacterial adhesion without killing by adhesion. There are three types of surfaces; Hydrogel surfaces, highly negatively charged surfaces, and ultra-hydrophobic surfaces. Hydrogel surfaces are

usually modified with hydrophilic polymers such as poly(ethylene glycol) (PEG) [11]. These polymers can form a hydration layer (**Figure 1.4c**). Highly negatively charged surfaces can prevent bacterial adhesion via electrostatic repulsion (**Figure 1.4d**). Finally, ultra- hydrophobic surfaces with low surface energy (hydrophobic) can also decrease bacterial adhesion [12] (**Figure 1.4e**).

1.3 Antimicrobial peptides

Antimicrobial peptides (AMPs) are peptides that can exhibit antibacterial, antifungal, antiparasitic, and antiviral activity. In 1939, gramicidin, an antimicrobial peptide that inhibits the growth of Gram-positive bacteria, was first reported. Most AMPs are produced by a number of organisms as a part of innate immune systems. However, many researchers are turning to non-natural sources to discover the next generation of AMPs. Antimicrobial peptides, both synthetic and natural, have a high diversity in sizes, sequences, and structures. An amphipathicity (positive charge and high density of hydrophobic residues) property of AMPs is important for their antibacterial activity.

1.3.1 Mechanisms of action

Some antimicrobial peptides (AMPs) are known to interact with intracellular targets such as inhibition of cell wall, DNA, RNA, or protein synthesis [13]. However, the main mechanism of AMPs involves their ability to cause cell membrane disruption and permeabilization, followed by cell lysis. Membrane permeation has been proposed to occur via one of three general mechanisms [14], [15] including barrel-Stave, toroid pore or wormhole, and carpet-like models (**Figure 1.5**).

1.3.1.1 Barrel-stave Model

For Barrel-Stave model, the process was initiated from an electrostatic interaction between positively charged peptides and negatively charged membrane components. Thus, AMPs bind electrostatically to the lipid head-group region of the bacterial membrane in an orientation parallel to the bilayer surface. The hydrophobic portion of the peptide is inserted into the hydrophobic core of the membrane and form transmembrane pores.

1.3.1.2 Toroid Pore or Wormhole Model

Initially peptides interact with the charged and hydrophobic bacterial membrane in an orientation that is similar to that proposed by the barrel-stave model. Then, the hydrophobic moieties of peptides displace the polar head groups, creating a breach in the hydrophobic region and inducing a curvature strain in the membrane and ultimately form a pore.

1.2.1.3 Carpet-like model

In this model, AMPs are intensively adsorbed onto the membrane and form peptide/lipid micelles, resulting in catastrophic collapse of membrane integrity with non-poration mechanism.

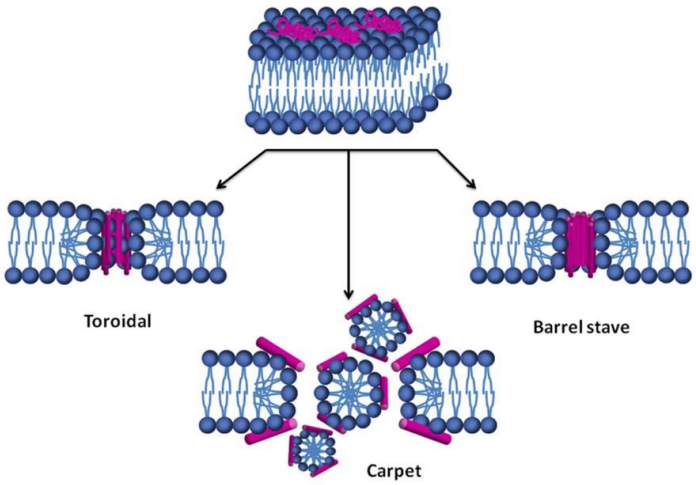

Figure 1.5 Different membrane-disruption models for antimicrobial peptides [16].

1.4 Biomaterials based on antimicrobial peptides

Owing to their low cytotoxicity, several biomaterials based on antimicrobial peptides were developed in recent years.

In 2008, Willcox and coworkers synthesized melamine peptide (TLISTWIKNKRKQRPRVSRRRRRRGGRRRR) via solid-phase peptide synthesis method. They also covalently immobilized these peptides onto commercial contact lens and compared antimicrobial activities of the covalently modified contact lens with peptides-adsorbed contact lens. The covalent coupling showed greater activity with

70%-reduction of bacterial adhesion in both Gram-negative (*Pseudomonas aeruginosa*) and Gram-positive bacteria (*Staphylococcus aureus*) [17].

In 2013, Kaiyang Lim and coworkers developed a tryptophan–arginine-rich synthetic peptide (CWR11, CWFWKWWRRRRR-NH_2) and immobilized it onto polydimethylsiloxane (PDMS) using polyethylene glycol (PEG) as a spacer. PEG can covalently conjugate the peptide to the allyl glycidyl ether (AGE) polymer brush and improve grafting efficiency onto PDMS surfaces (**Scheme 1.1**). CWR11-immobilized PDMS slide surfaces showed excellent antibacterial activity against *E. coli*, *S. aureus*, and *P. aeruginosa* [18].

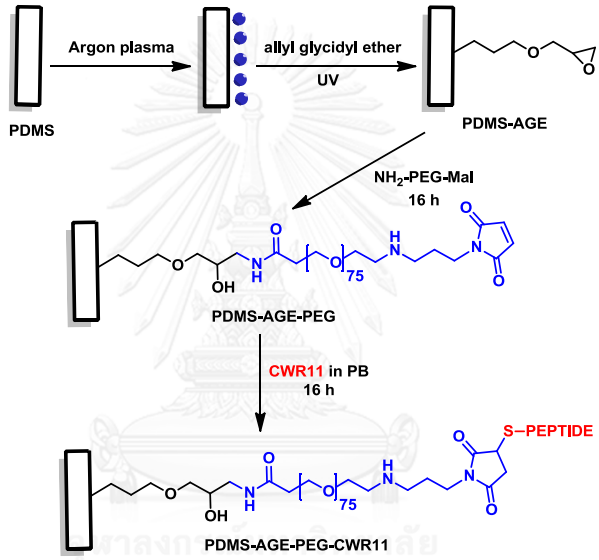

Scheme 1.1 Immobilization of CWR11 peptide on PDMS surface.

In 2014, Etayash and coworkers synthesized Leucocin A (LeuA) with 37 amino acid residues (NH_2-KYYGNGVHCTKSGCSVNWGEAFSAGVHRLANGGNGFW-COOH) using standard Fmoc solid-phase peptide synthesis by automatic peptide synthesizer. LeuA was covalently conjugated to functionalized gold substrates through N-terminus and C-terminus. The peptide-immobilized surface through C-terminus showed higher binding to bacteria *Carnobacterium divergens* LV13 than did the N-terminus modification (**Scheme 1.2**) [19].

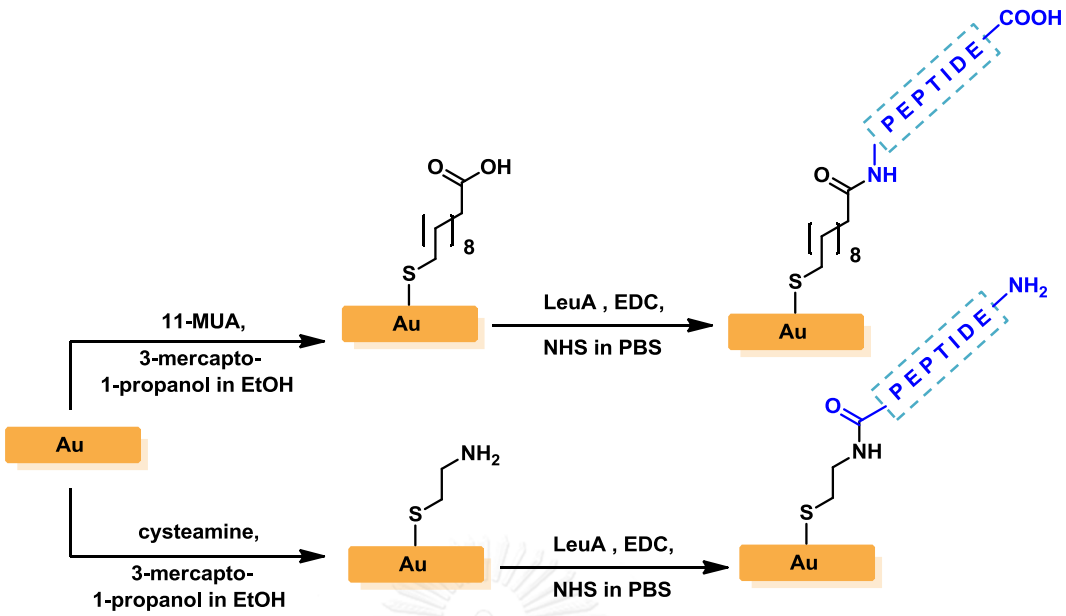

Scheme 1.2 Immobilization of LeuA peptide on gold surface.

In 2009, Hancock and coworkers reported a fabrication of surface-tethered cationic peptides onto cellulose support. The 12-mer peptide (RRWKIVVIRWRR) were immobilized on cellulose surface via cellulose-amino-hydroxypropyl ether (CAPE) linker. They found antibacterial effects of the peptide-modified cellulose against *Pseudomonas aeruginosa* [20]. The D-9-mer peptide (RLYLRIGRR), the modified sequence from the active site of a beetle defensin, was immobilized to amino-functionalized cotton fibers by using the SPOT synthesis technique to give an antimicrobial surface against Methicillin-resistant *Staphylococcus aureus* (MRSA) (**Scheme 1.3**) [21].

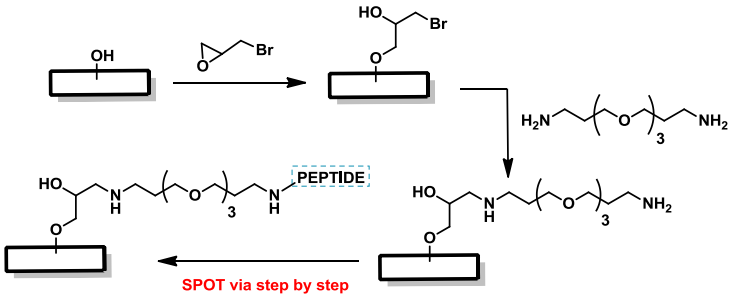

Scheme 1.3 Immobilization of D-9mer peptide onto cotton fibers.

1.5 Cellulose

Cellulose is the most abundant natural biomaterials with low toxicity and biocompatibility. Cellulose is a linear homopolymer composed of D-anhydroglucopyranose unit (AGUs), that are joined together with beta-1,4-glycosidic bonds between the C4 carbon atom and the C1 carbon atom (**Figure 1.6**). The hydroxyl groups at 2, 3 and 6 positions are responsible for the reactions of cellulose. However, the reactivity of the hydroxyl groups can be expressed as OH–C6 > OH–C2 > OH–C3 [22].

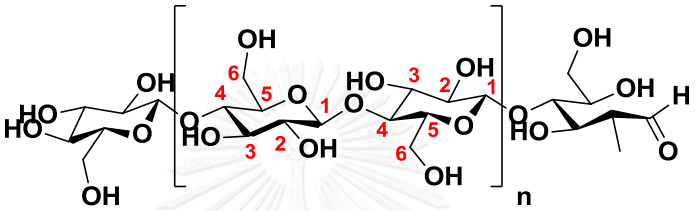

Figure 1.6 The molecular structure of cellulose.

Cotton fabrics, produced from natural cellulosic fibers, were widely used in many health-care applications. However, cotton fabrics do not have antibacterial properties by themselves due to their hydroscopic properties, which contribute to their strong moisture-absorbing abilities that are an ideal condition for the growth of bacteria.

1.6 Aim of research

Due to the fact that attachment of bacteria on biomaterial surface is the first step towards infections in human, the development of novel antibacterial surfaces could drastically reduce infections and consequent complications. In this study, contact-active antimicrobial surfaces were synthesized by introducing short peptides (RRGIR) on cotton fabrics. The further modification occurred with the attachment of aliphatic acids with different lengths (C4, C6, C10, C12, C16, and C18) to the short peptides via SPOT method.

1.6.1 The objective of this research

1. To develop a novel antibacterial surfaces by immobilizing short peptide on cotton surfaces.
2. To evaluate antibacterial activities of modified surfaces against Gram-positive and Gram-negative bacteria.
3. To evaluated the biocompatibility of the modified cotton surfaces against L929 mouse fibroblast cell line.

CHAPTER II

EXPERIMENTAL SECTION

2.1 Chemicals and materials

Fmoc protected L- and D-amino acids were purchased from GL Biochem (Shanghai, China) and Chem-Impex International (USA). All other reagents for peptide synthesis were obtained from Merck and Sigma Aldrich (**Table 2.1**). Anhydrous *N,N*-dimethylformamide (H_2O ≤ 0.01 %, DMF) for peptide synthesis was obtained from RCI Labscan (Thailand) and dried over activated 4 Å molecular sieves before use. Methanol, Dichloromethane and *N,N*-dimethylformamide for washing the solid supports were purchased from RCI Labscan and used without further purification. Milli-Q water was obtained from ultrapure water system with Millipak® 40 filter unit 0.22 µm, Millipore (USA). The solid support for peptide synthesis is cotton fabrics purchased from Thai Textile Development and Finishing co., ltd. Nutrient Broth and Agar powder were purchased from HiMedia.

Table 2.1 Structure of protected amino acids and linear fatty acids for the preparation of solid phase peptide synthesis.

Compound	Molecular weight	Structure
Fmoc-Arg(Pbf)-OH	648.77	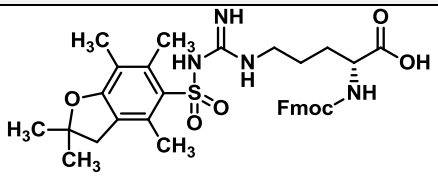
Fmoc-Gly-OH	297.31	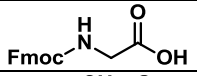
Fmoc-Ile-OH	353.41	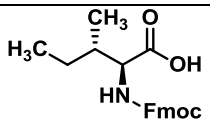
Fmoc-Leu-OH	353.41	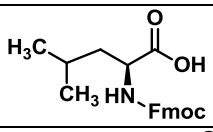
Fmoc-Tyr(tBu)-OH	459.53	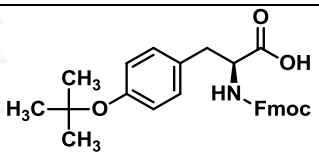
Butanoic acid	88.11	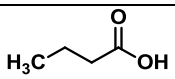
Hexanoic acid	116.16	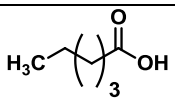
Decanoic acid	172.26	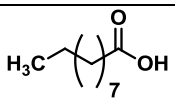
Dodecanoic acid	200.32	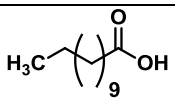
Palmitic acid	256.42	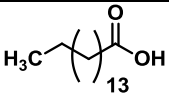
Stearic acid	284.48	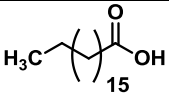

2.2 Instruments and Equipment

All compounds were weighed on an electrical balance (model TP-214, Denver Instrument Gmbh, Göttingen, Germany). Sample surfaces were shaken on rotary shaker (KS 130 basic, IKA®-Werke GmbH & CO. KG, Germany)

Mass data of peptides and lipopeptides were obtained from a Bruker Microflex Matrix Assisted Laser Desorption Ionization Time-of-Flight Mass Spectrometer (MALDI-TOF-MS). Samples were prepared and deposited onto a stainless steel target substrate.

The UV-Visible absorption spectra were recorded at room temperature in a standard 1 cm quartz cuvette using a Varian Cary 100 Bio UV-Visible Spectrophotometer. The deuterium and the visible lamps were used as light sources.

2.3 Synthesis of lipopeptides on cellulose

Peptides and lipopeptides were immobilized to the cotton fabrics with and without flexible molecular spacer chains by coupling the carboxyl group or C-terminus of one amino acid to the amino group or N-terminus of another directly on the cotton surfaces using standard Fmoc-strategy. An overall synthesis plan is shown in **Scheme 2.1** and **Table 2.2**.

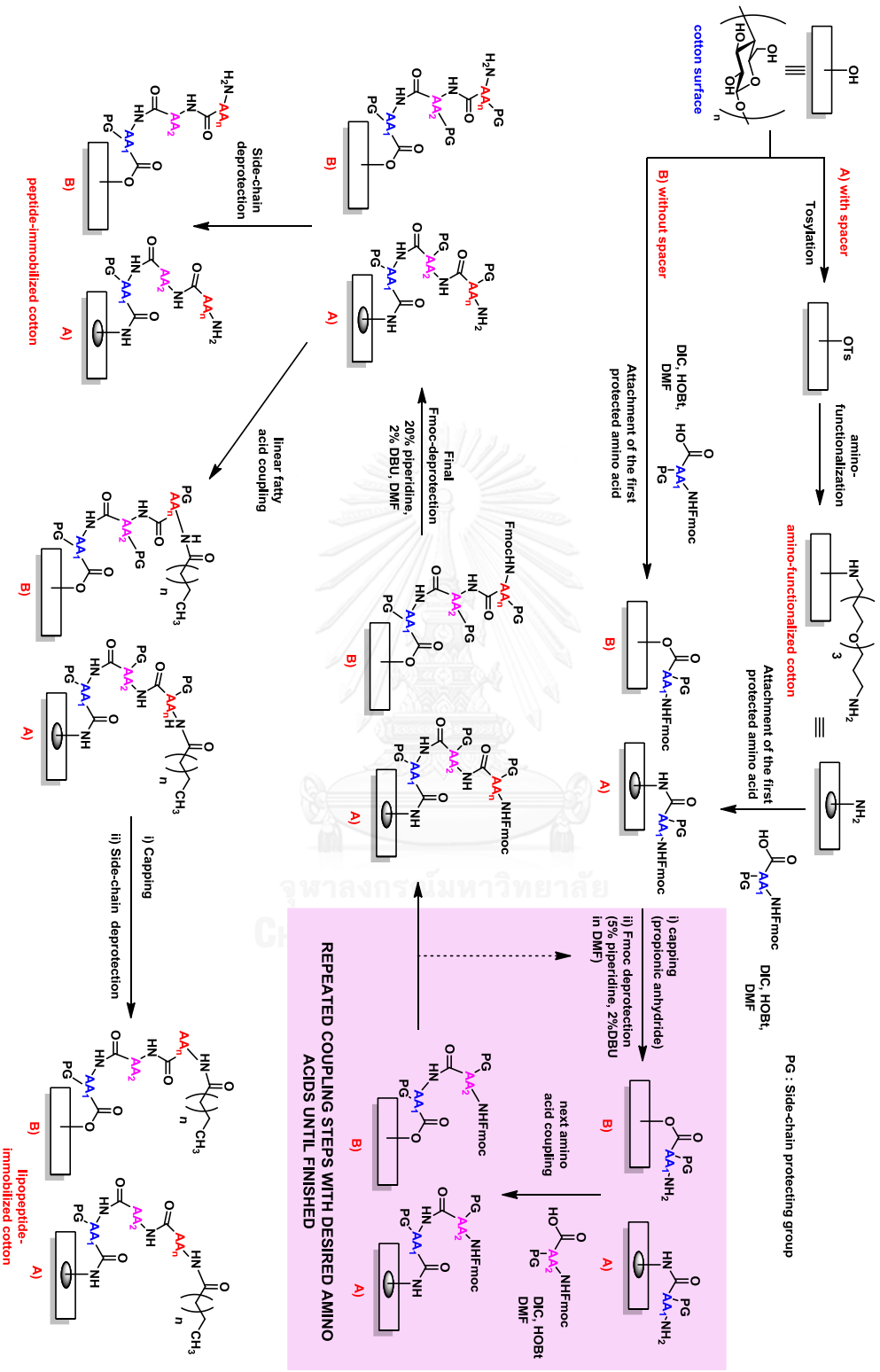

Scheme 2.1 An overall synthesis plan of peptides and lipopeptides-immobilized cottons.

Table 2.2 List of peptide sequences.

Name	Sequence	
	with spacer	without spacer
D, L-9mer	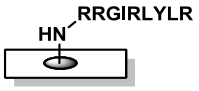	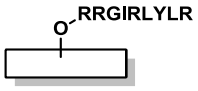
5mer	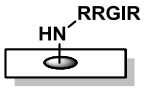	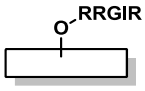
5mer.C4	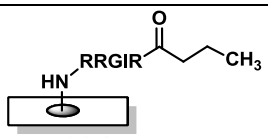	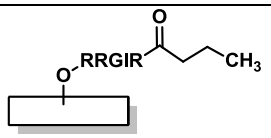
5mer.C6	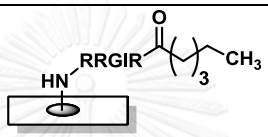	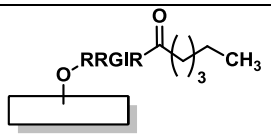
5mer.C10	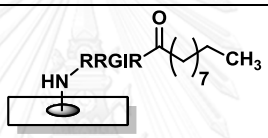	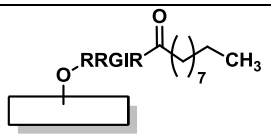
5mer.C12	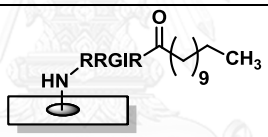	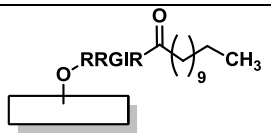
5mer.C16	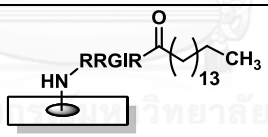	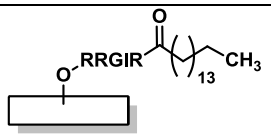
5mer.C18	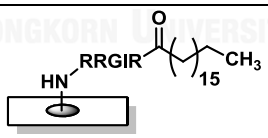	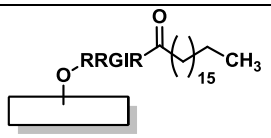
C12	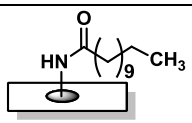	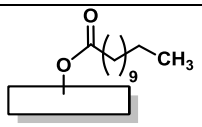
C16	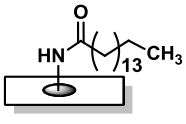	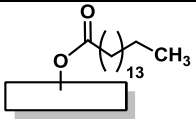
C18	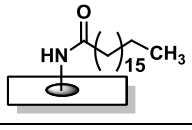	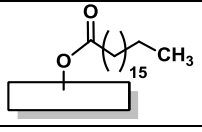

2.3.1 Preparation of Cotton cellulose surfaces

Cut a piece of cotton fabrics to the size 6x6 cm^2, 1x1 cm^2 grids were then drawn on each piece and mark the synthesis positions at the center of each grid with a pencil (**Figure 2.1**). Next, cotton fabrics were washed with 1:1 *N,N*-dimethylformamide (DMF) : deionized water (H_2O) (2x, 5 min each), methanol (5 min), and dichloromethane (5 min), followed air drying at room temperature.

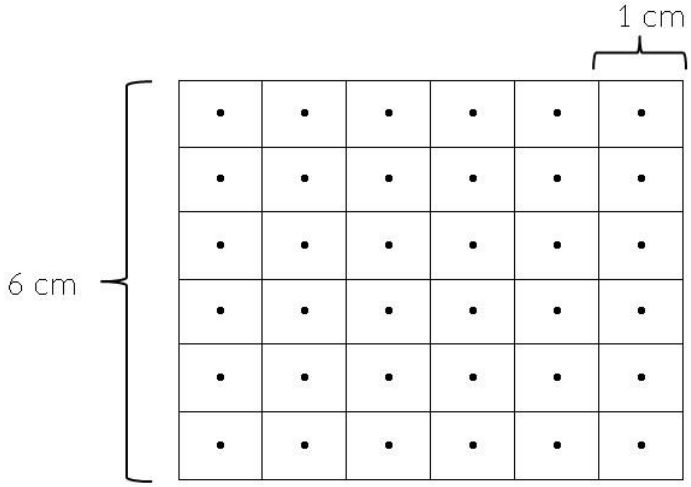

Figure 2.1 Pattern for synthesis of peptide on cotton fabric.

2.3.2 Preparation of amino-functionalized cotton fabrics

In the case of cotton fabrics with flexible molecular spacer chains, each of cotton fabric was tosylated in 2 M TsCl (20 mmol) in pyridine (10 mL) for 90 min (shaking at 160 rpm) and subsequently washed with DMF (2x, 5 min each), methanol (5 min), and dichloromethane (5 min) and air-dried. Thereafter, the tosylated cotton fabrics was converted to the amino group by immersing in a solution of 1 M 4,7,10-trioxatridecane-1,13-diamine (10 mmol) in DMF (10 mL) at room temperature for 18 h (shaking at 160 rpm). The amino-functionalized cotton fabrics were washed with 5 M NaOH in 7:1 MeOH:H_2O (1x 5 min), MeOH (1x, 5 min), DMF (1x, 5 min), and water (2x, 5 min each), respectively and then heated at 40°C for 18 h.

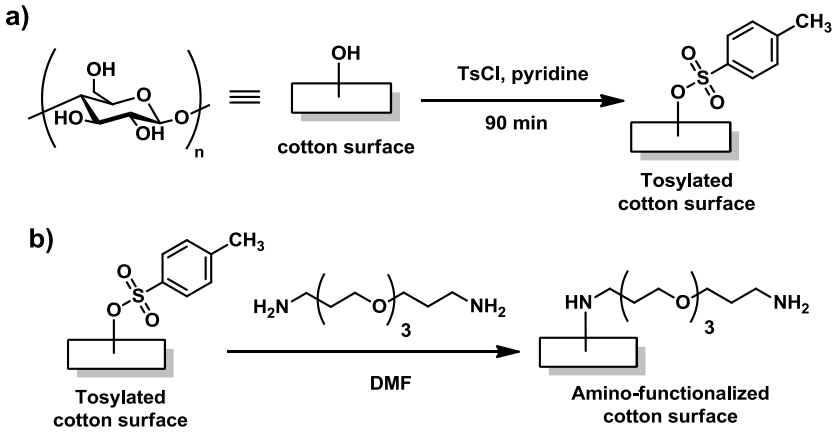

Scheme 2.2 Synthesis of a) tosylated and b) amino-functionalized cotton surface.

2.3.3 Synthesis of peptide and lipopeptides on cellulose surfaces

Peptides and lipopeptides were synthesized onto amino-functionalized and untreated cotton fabrics via standard Fmoc-based strategies. The process usually consists of three steps;

2.3.3.1 Attachment of an amino acid to the amino-functionalized or untreated cotton fabrics with carbodiimide coupling:

Fmoc-amino acid (0.45 M) and 1-hydroxybenzotriazole hydrate (HOBt, 0.9 M) were dissolved in anhydrous DMF and then *N,N'*-diisopropylcarbodiimide (DIC, 1.35 M) was added to the solution. The solution was directly spotted (2 µL) onto the amino-functionalized and untreated cotton surfaces at marked positions. The sheet was kept at room temperature for 10 min. This process was repeated two more times. After the reaction, the surfaces were washed with 1:1 DMF:H_2O (2x, 3min) to remove unreacted Fmoc-amino acid. The attachment reactions are shown in **Scheme 2.3**.

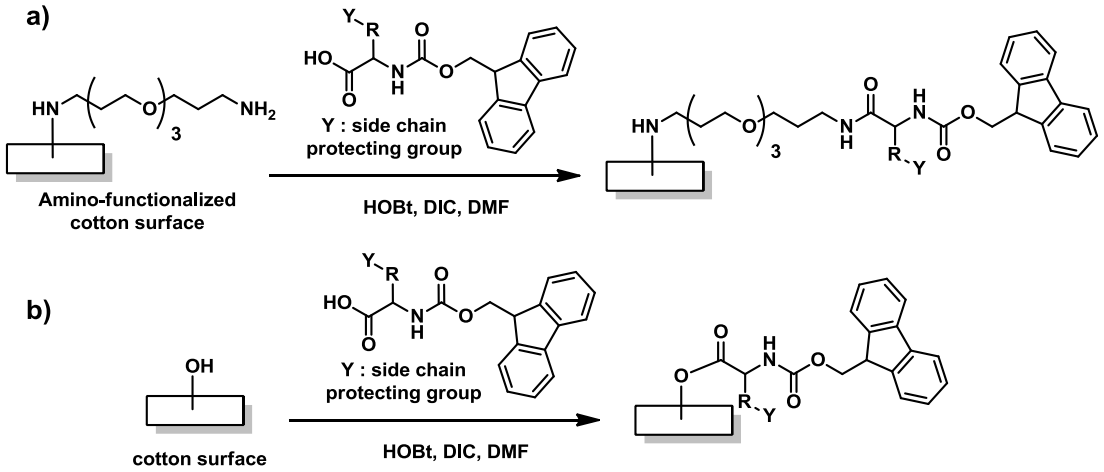

Scheme 2.3 Attachment of the first N^{α}-protected amino acid to a) amino-functionalized cotton surface and b) untreated cotton surface.

2.3.3.2 Capping step (blocking unreacted free amino groups):

Place the membranes from the previous step in the solution of 5% propionic anhydride (0.5 mL) in DMF (9.5 mL) for 15 min at room temperature (shaking at 160 rpm). The surfaces were washed with 1:1 DMF:H_2O (3 min, 2x), and MeOH (3 min, 1x), respectively. The cotton surfaces were air-dried at room temperature. The reaction is shown in **Scheme 2.4**. Note that there may also be unreacted amino groups from the amino acid at each cycle – this is also expected to react with propionic anhydride too.

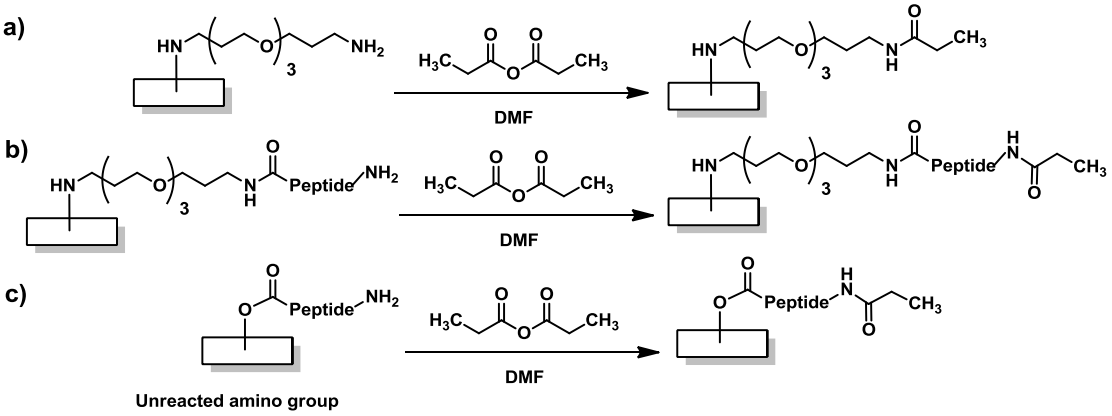

Scheme 2.4 capping of the unreacted amino group.

2.3.3.3 Fmoc-deprotection step:

Fmoc group was removed by immersing into a solution of 5% piperidine (0.5 mL) and 2% DBU (0.2 mL) in DMF (9.3 mL) for 15 min with shaking at 160 rpm to allow the next amino acid of the sequence to be attached. After washing with 1:1 DMF:H_2O (3 min, 2x), MeOH (3 min, 1x), the cotton sheet was air-dried at room temperature. The reaction is shown in **Scheme 2.5**.

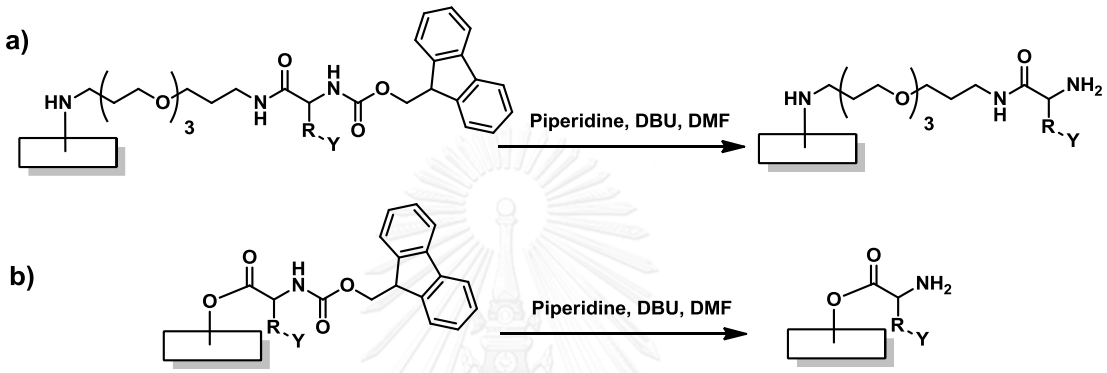

Scheme 2.5 Deprotection of Fmoc group of Fmoc amino acid-immobilized cotton a) with spacer and b) without spacer .

The cycle is repeated until the sequence is complete. The final Fmoc group was carried off with the solution of 20% piperidine (2 mL) and 2% DBU (0.2 mL) in DMF (7.8 mL) for 15 min with shaking at 160 rpm. The peptide-immobilized cotton surfaces were subsequently washed with 1:1 DMF:H_2O (3 min, 2x), MeOH (3 min, 1x), and air-drying.

For lipopeptides-immobilized cotton, a fatty acid was coupled as described in step **Figure 2.6**, followed by capping using the same capping condition.

2.3.3.4 Linear fatty acid coupling:

The short peptides from previous step were conjugated with a linear fatty acid via carbodiimide coupling (**Scheme 2.6**). A solution of aliphatic acids with different lengths (C4, C6, C10, C12, C16 and C18) was coupled onto the cotton sheet using the same coupling condition as the amino acid coupling,

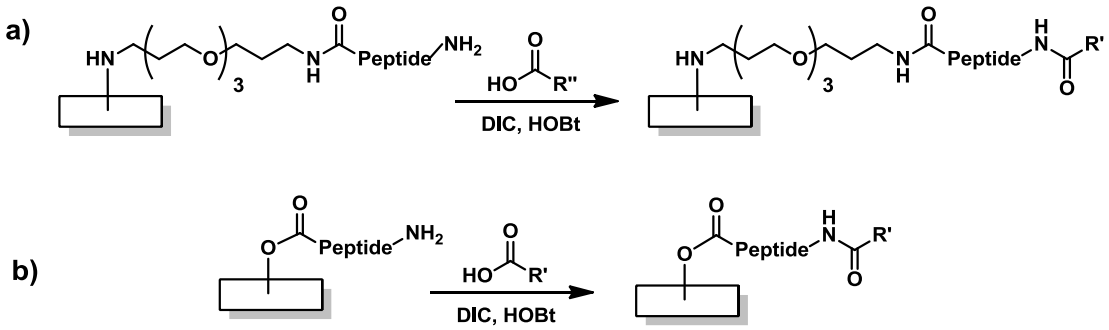

Scheme 2.6 Linear fatty acid coupling

2.3.4 Side-chain protection group cleavage

Finally the side-chain protecting group was removed in acid solution (90% TFA : 1% phenol : 2%H_2O : 3% triisopropylsilane : 4% CH_2Cl_2) for 30 min and then 3-h incubation in 50% TFA : 1% phenol : 2% H_2O : 3% triisopropylsilane : 44% CH_2Cl_2. The functionalized cotton fabrics were then rinsed using CH_2Cl_2 (3x, 5 min each), MeOH (3x, 5 min each) and H_2O (multiple times). Thereafter, the functionalized cotton sheets were air-dried at room temperature.

2.4 Surface characterization

2.4.1 Determination of the loaded amino group of amino functionalized surfaces

The quantification of amino functional groups on the amino-functionalized cotton fabric was performed using a colorimetric assay. The amino-functionalized cotton fabrics (2.5x2.5 cm^2) were immersed in an aqueous solution of 4-(2-hydroxy-1-naphthylazo)benzano-sulfonic acid) sodium salt (CI Orange 7, 25 mg) in acetic acid (475 µL) for 30 min at 50°C. After rinsed with H_2O to remove unbound dye, the samples were immersed in 25% aqueous pyridine solution. The absorbance of the cleaved dye solution was then measured at 485 nm with CARY 100 Bio UV-Visible spectrophotometer (Varian Inc., USA).

2.4.2 Determination of the Loaded Peptide

The amount of peptide per spot was determined by quantification of the dibenzofulvene chromophore that was cleaved off during Fmoc N^{α}-deprotection steps. A hole-punched fabric was immersed in a solution of 20% piperidine (100 µL) and 2% DBU (10 µL) in DMF (390 µL) for 15 min. The absorbance of the cleaved fulvene solution was measured using the molecular extinction coefficient (**ε**) of 4.6594 $mM^{-1}cm^{2}$ at 296 nm.

2.4.3 Scanning Electron Microscopy (SEM) analysis

The morphological changes of the peptide-immobilized cotton fabrics were observed by using a JSM-6480LV Scanning Electron Microscope (JEOL Ltd.). The surfaces were mounted on a metal stub and sputtered with gold to make the sample electrical conductive.

2.4.4 MALDI-TOF Mass spectrometry

To characterize the peptides with MALDI-TOF Mass spectrometry, Fmoc-Rink amide linker (4-[(2,4-dimethoxyphenyl)-(Fmoc-amino)methyl]phenoxy-acetic acid) was inserted between the spacer and the first amino acid by carbodiimide coupling (**Scheme 2.7**). The modified peptides that were synthesized via Rink amide linker were cleaved from the cotton fabrics using TFA-Scavenger (88% TFA, 5% phenol, 5% water, 2% TIPS) for 2 hours and analyzed by MALDI-TOF Mass Spectrometry. The samples were prepared by mixing 1 µL of samples with 10 µL of matrix solution containing α-cyano-4-hydroxycinnamic acid (CCA) in 0.1% trifluoroacetic acid in acetonitrile:water (1:2) solution and deposited on a metal target. The mass spectra of lipopeptide were recorded on Microflex MALDI-TOF mass spectrometer (Bruker Daltonics).

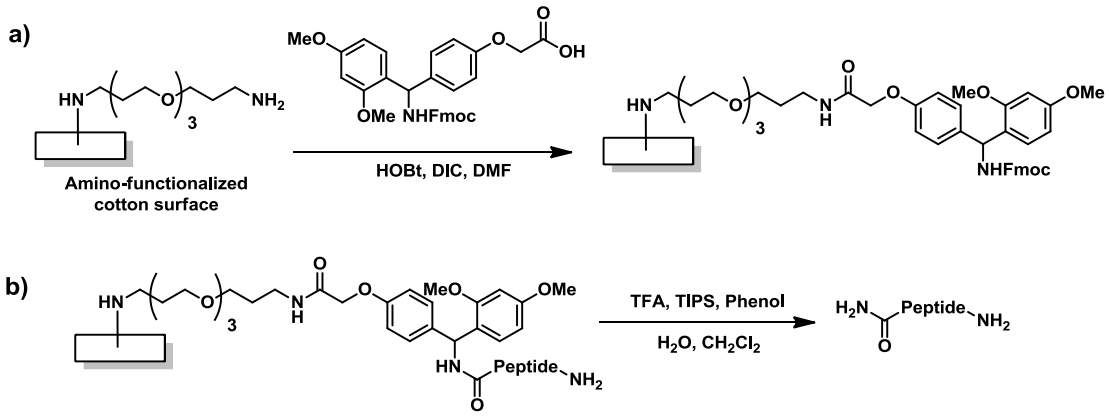

Scheme 2.7 Attachment of Fmoc-Rink amide linker to a) the amino functionalized surface and b) the detachment of peptide from the surface.

2.5 Antibacterial activity of peptides and lipopeptides-immobilized surfaces.

2.5.1 Bacterial culture

A single colony of the bacteria (*Staphylococcus aureus*-ATTC 6538P, *Escherichia coli-ATCC* 8739 or *Pseudomonas aeruginosa*-ATCC 9027) was inoculated into 50 ml of sterile Nutrient broth (NB) and incubated at 37°C on a shaker (200 rpm) for 18 hours.

2.5.2 The antibacterial assay

For testing the efficacy of antibacterial textiles, the cotton fabrics were quantitatively tested for bacterial growth inhibition against Gram-positive bacterium (*Staphylococcus aureus*-ATTC 6538P) and Gram-negative bacteria (*Escherichia coli*-ATCC 8739 and *Pseudomonas aeruginosa*-ATCC 9027) using the Japanese Industrial Standard (JIS) L 1902 method. An overnight culture of *S.aureus*, *E.coli* or *P.aeruginosa* (1 mL) was added to 100 mL of sterile Nutrient Broth (NB). After the suspension was incubated at 37 °C with shaking at 200 rpm, the cell density of bacteria suspensions was determined by measuring the optical density (OD620) to mid-exponential phase bacteria using BioMATE S3 Spectrophotometer. The inoculum suspension was diluted to approximately $1x10^7$ CFUs/mL with sterile normal saline solution (NSS, 0.85% wt/v, NaCl). The functionalized cotton fabric was inoculated with 100 µL aliquots of the appropriate dilution of bacterial suspension for 18 hours at 37°C. Bacterial

colonies were counted on each plate and the number was used to calculated the number of bacteria (CFU) per milliliter as shown in the equations below.

$$\text{Individual dilution factor} = \frac{\text{Volume transferred}}{\text{Total volume in tube}}$$

$$\text{CFU/mL} = \frac{\text{Number of colonies per mL plated}}{\text{Total dilution factor}}$$

2.6 Biocompatibility assay

2.6.1 Cell culture

L-929 mouse connective tissue fibroblast (DSMZ ACC 2) cell lines were cultivated in Roswell Park Memorial Institute medium (RPMI) with 10% Fetal Bovine Serum (FBS). Incubation conditions were kept constant at 37°C in 5% CO_2 and humidified atmosphere.

2.6.2 Cytotoxic testing

To determine cell viability, the colorimetric MTT metabolic activity assay was used L-929 mouse fibroblasts from stock cultures were trypsinized and diluted to a concentration of $4x10^5$ cells/mL with cell culture medium (RPMI with 10% FBS). All samples were immersed in 70% EtOH overnight. After the ethanol was removed, the samples were dried at room temperature and placed in 24-well plates. 50 µL of approximately $4x10^5$ cells/mL of L-929 mouse fibroblast was seeded onto each sample and incubated for 2 h at 37 °C in 5% CO_2 humidified atmosphere. Then, 500 µL of RPMI medium was added to each well and incubated for different time periods (24, 48 and 72 hours). The culture media were replaced with 300 µL of 0.5 mg/mL MTT (3-(4,5-dimethylthiazol-2-yl)-2,5-diphenyltetrazolium bromide) in 0.9% NSS and incubated for an additional 2 h at 37°C. The MTT formazan granules (purple precipitate) were formed and 300 µL of DMSO was added to dissolve this formazan product. The absorbance measurements were taken at 540 nm using Multiskan FC microplate reader. Experiments were performed in triplicate. Optical density was used to calculate the percentage of cell viability with the following formula:

$$\% \text{ cell viability} = \frac{\text{OD treatment}}{\text{OD control}} \times 100$$

CHAPTER III

RESULTS AND DISCUSSION

3.1 Concept of molecular design

Based on the discussion in chapter I, it can be assumed that the amphipathic property of AMPs is the key to designing novel peptides with increased potency. Owing to this reason, this research aimed to design novel antimicrobial surfaces through chemically modified cotton with a short antimicrobial peptide that was conjugated with linear fatty acids to increase the hydrophobicity via the SPOT method and standard Fmoc chemistry.

3.2 Synthesis of lipopeptides on Cellulose

An overall synthetic plan is shown in **Figure 3.1**. The peptides and lipopeptides were synthesized and immobilized step-by-step with C-to-N direction using SPOT-synthesis technique on the cotton fabrics. This study also incorporates a comparative study where an amino spacer was used or omitted in order to study the influence of the spacer on antibacterial activity. The detail of synthesis is described below.

AMPs with spacer. The first amino acid was coupled by DIC/HOBt coupling onto amino-functionalized cotton, which was previously converted from the hydroxyl group of untreated cotton to amino-functional group with a hydrophilic spacer. After capping step with propionic anhydride, the Fmoc group was deprotected using DBU/piperidine to expose the free amino group for the next cycle of amino acid addition. This process was repeated until finished. In the case of **D-9mer**, **9mer** and **5mer**-peptide-immobilized surface, the final step was side-chain deprotection under acidic condition. On the other hand, **5mer.R'** surfaces were prepared by capping the last amino acid with a linear carboxylic acid with varying chain lengths via a standard DIC/HOBt coupling, followed by the side-chain deprotection. In addition, cotton fabrics were directly coupled with fatty acids as a controls (**R'**).

AMPs without spacer. The process was the same as the first type, except that the first amino acid was coupled directly to the hydroxyl group of cellulose, thus generating **9mer**, **5mer**, **5mer.R'**, and **R'** surfaces.

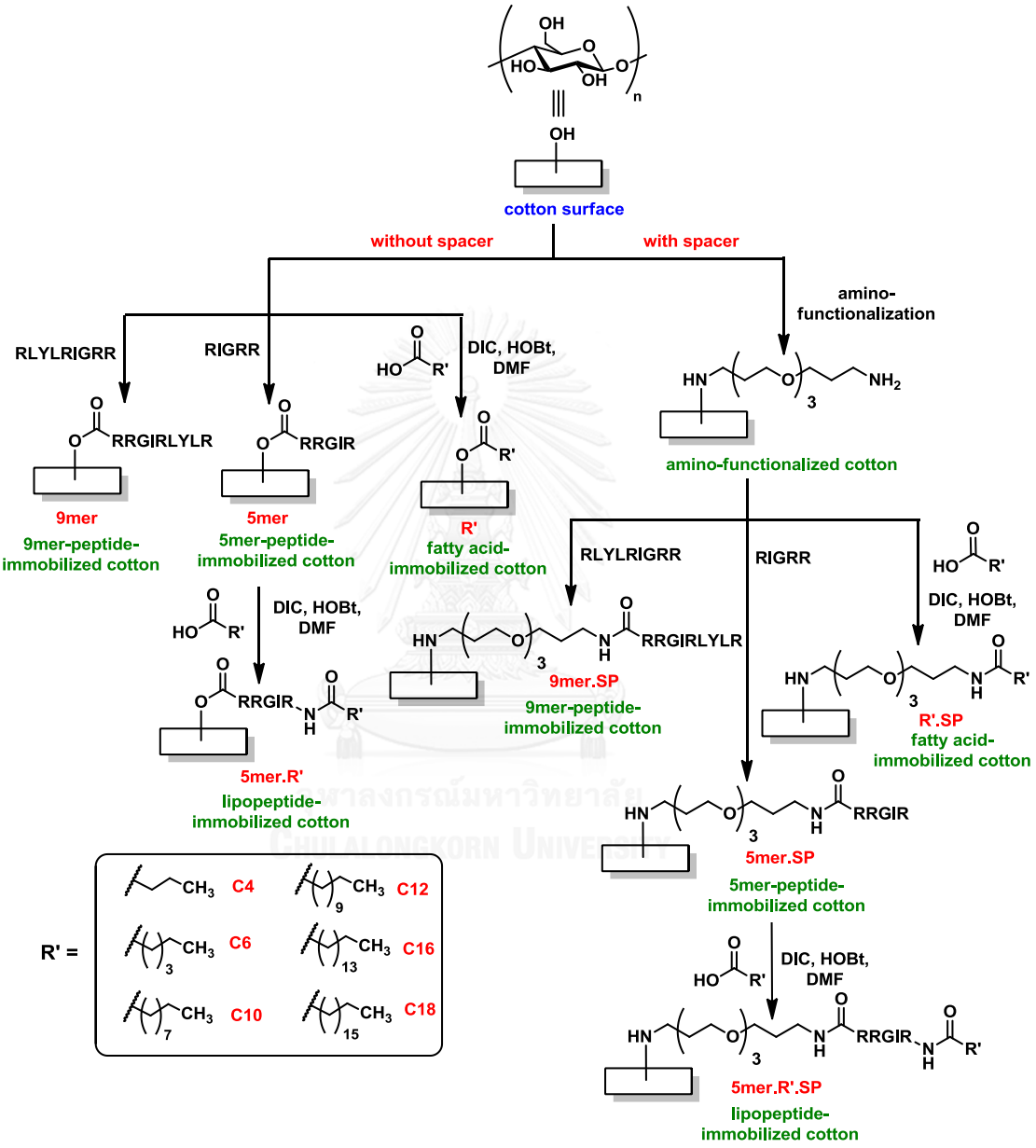

Figure 3.1 The overall synthesis plan of peptides and lipopeptides-immobilized cotton surfaces.

3.2.1 Preparation of amino-functionalized cotton fabrics

Cotton fabric was tosylated in 2 M TsCl in pyridine. The hydroxyl group, which is a poor leaving group for substitution reactions, was converted to sulfonate group (a good leaving group) by treating with *p*-toluenesulfonyl chloride in the presence of pyridine as a weak base and nucleophilic catalyst (**Figure 3.2**).

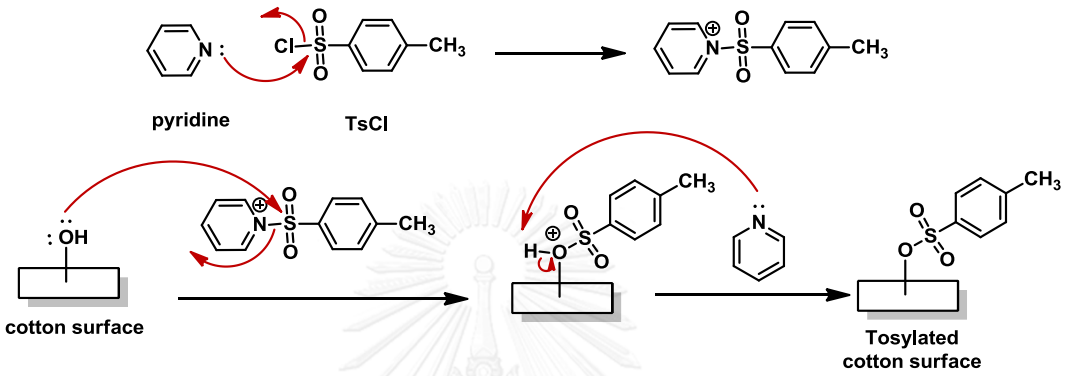

Figure 3.2 Mechanism of Tosylation reaction.

Tosyl group was then substituted by 4,7,10-trioxatridecane-1,13-diamine to make an amino group available (**Figure 3.3**).

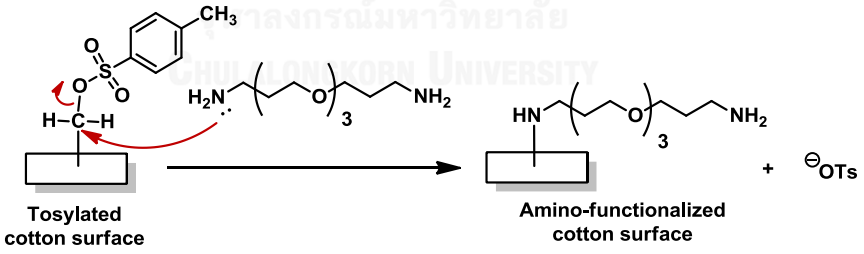

Figure 3.3 Functional group interconversion of tosylated group to amino group.

3.2.2 Synthesis of peptide and lipopeptides on cellulose surfaces

3.2.2.1 Attachment of an amino acid to the amino-functionalized or untreated cotton fabrics with carbodiimide coupling:

The first amino acid was immobilized on amino-functionalized cotton and untreated cotton. Under the standard carbodiimide condition, the carboxyl group from the amino acid and the surface amine (or alcohol) were reacted to form the amide (ester) bonds.

The carboxyl group of the amino acid was activated with DIC and gave O-acylisourea as a product. The O-acylisourea was reacted with 1-hydroxybenzotriazole (HOBt) to form an activated ester that reacted with the hydroxyl group or the amino group of untreated and amino-functionalized cottons, respectively (**Figure 3.4**). The HOBt was added to reduce epimerization and isomerization to N-acylurea (**Figure 3.5**) [23].

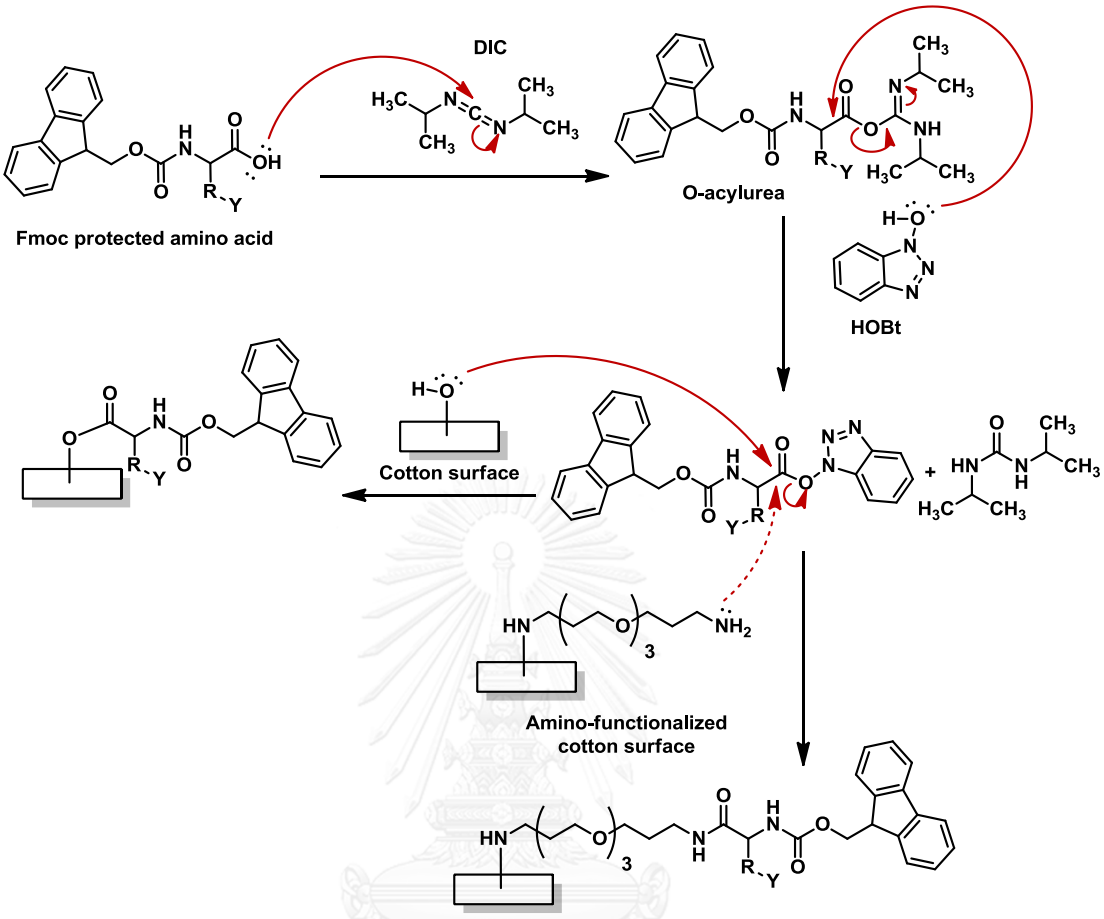

Figure 3.4 Mechanism of DIC/HOBt coupling.

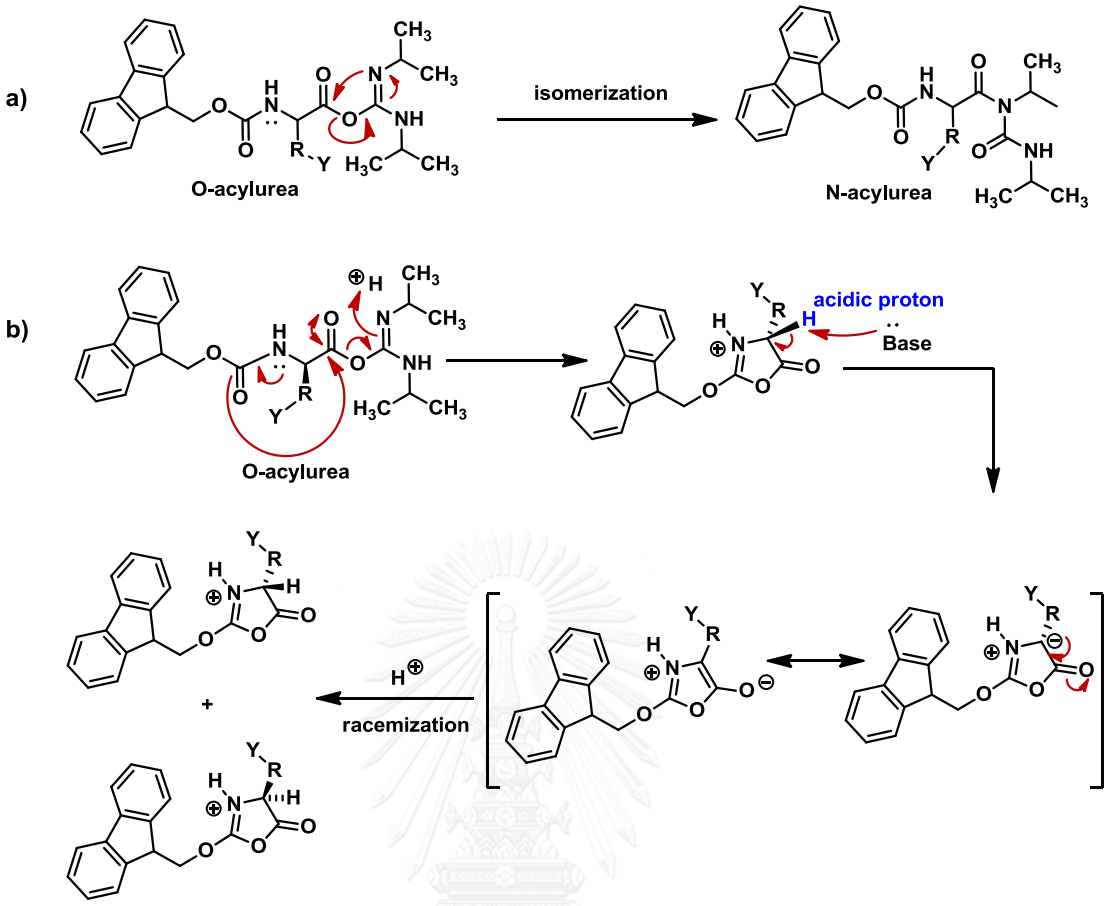

Figure 3.5 Mechanism of a) isomerization and b) epimerization of O-acylurea.

3.2.2.2 Capping step (blocking unreacted free amino groups):

The unreacted amino group was subsequently capped by acylation with propionic anhydride to reduce the generation of truncated peptide (**Figure 3.6**).

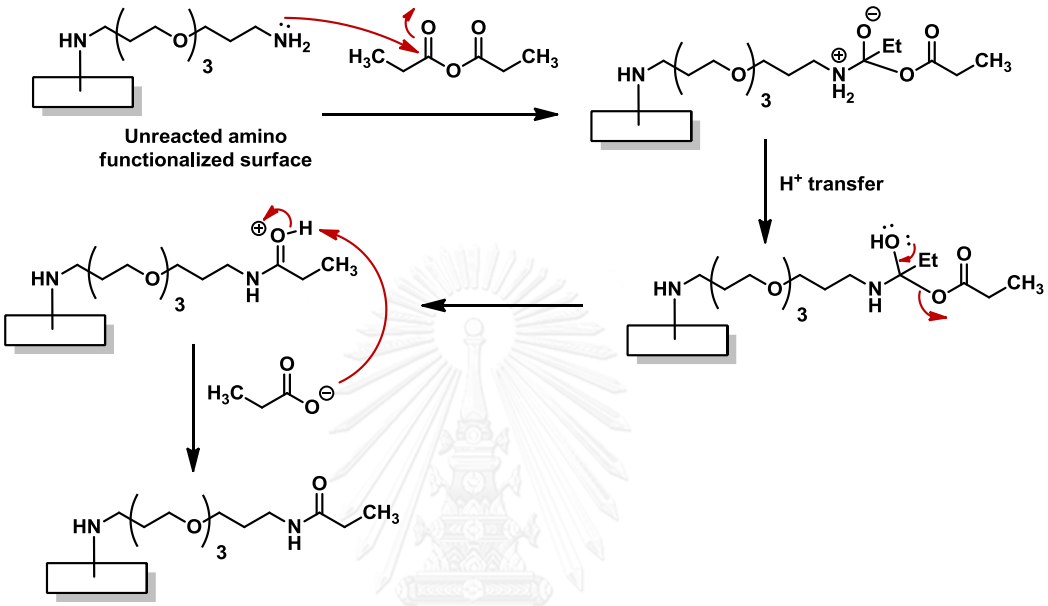

Figure 3.6 Mechanism of acetylation reaction of the unreacted amino group.

3.2.2.3 Fmoc-deprotection step:

The α-amino group of amino acids was protected by 9-fluorenylmethyloxycarbonyl (Fmoc) group. To allow the next amino acid of the sequence to be attached, the Fmoc group was removed with the solution of 5% piperidine and 2% DBU (**Figure 3.7**). Fmoc group with the lone hydrogen on the β-carbon is acidic, therefore, it was rapidly removed by weak bases in polar medium (DMF). During the deprotection step, piperidine or DBU deprotonates the fluorene ring to generate a cyclopentadiene-like intermediate and lead to dibenzofulvene. Dibenzofulvene was scavenged by piperidine to form dibenzofulvene piperidine adduct.

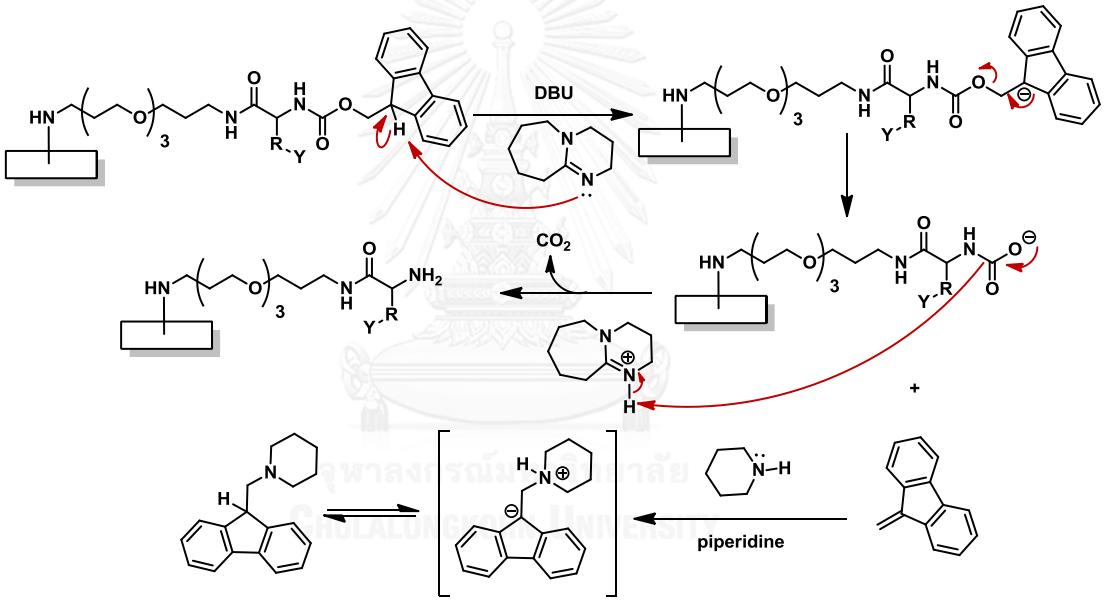

Figure 3.7 Mechanism of Fmoc removal with piperidine and DBU.

Next amino acids were coupled with the same condition of cycle (a-c). The cycle is repeated until the sequence is complete. Final Fmoc group was deprotected with the solution of 20% piperidine and 2% DBU, thereby generating peptide-immobilized cotton without cleavage of side-chain protecting groups.

3.2.2.4 linear fatty acid coupling:

For lipopeptide-immobilized cotton surfaces, after Fmoc group was deprotected in final step, linear fatty acids (C4, C6, C10, C12, C16, and C18) was conjugated to a short peptide (RIGRR) via DIC/HOBt coupling to increase the hydrophobicity, followed by a blocking step with a propionic anhydride.

3.2.2.5 Side-chain protection group cleavage:

Side-chain protecting groups of peptide and lipopeptide immobilized cotton were cleaved under acidic condition, thereby generating the **D-9mer**, **9mer** and **5mer** peptide-immobilized cottons.

The side-chain protecting groups of Arginine (Arg) and Tyrosine (Tyr) are pentamethyl-2,3-dihydrobenzofuran-5-sulfonyl (Pbf) and tert-Butyl (tBu) groups, respectively. Cleavage of the side-chain protecting group was accomplished using TFA-scavenger.

In the first step, the oxygen atom of tert-butyl group was protonated to give an oxonium ion intermediate. Thereafter, a stable tert-butyl carbocation was generated. The carbocation was trapped with phenol or triisopropylsilane as a carbocation scavenger to prevent alkylation (**Figure 3.8a**). In addition, cleavage of Pbf group was accomplished using the same condition (**Figure 3.8b**).

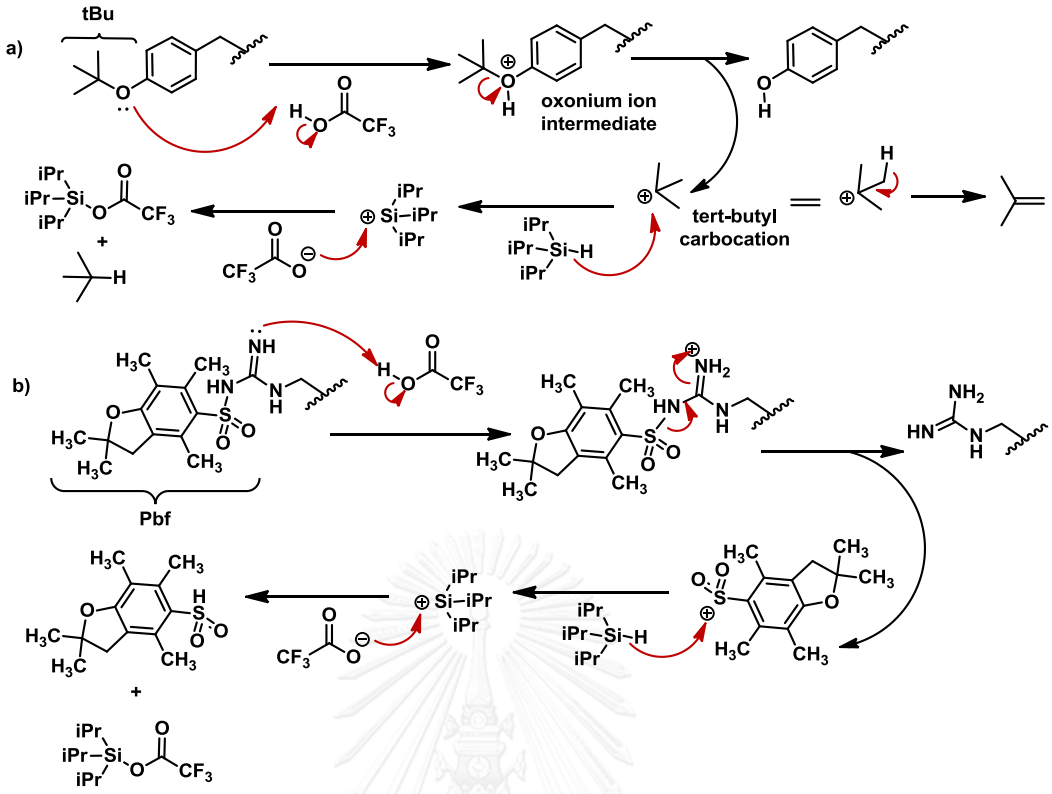

Figure 3.8 Mechanism for the cleavage of (a) tert-butyl and (b) Pbf group.

3.2.3 Surface characterization

3.2.3.1 Determination of the loaded amino group of amino functionalized cotton.

The amount of the amino-terminal spacer chain loaded on the cotton surface was determined via colorimetric assay based on the reversible electrostatic interaction between the negatively charged sulfonated dye CI Acid Orange 7 and the positive charge of protonated amino group in acidic condition of aqueous acetic acid. In the alkaline condition of aqueous pyridine solution, CI Acid Orange 7 was released as shown in **Figure 3.9**. The solution was measured with a UV/Vis spectrophotometer at 485 nm. The amount of CI Acid Orange 7 dye released to the solution is proportional to the amount of the amino loaded on the cotton surface [24].

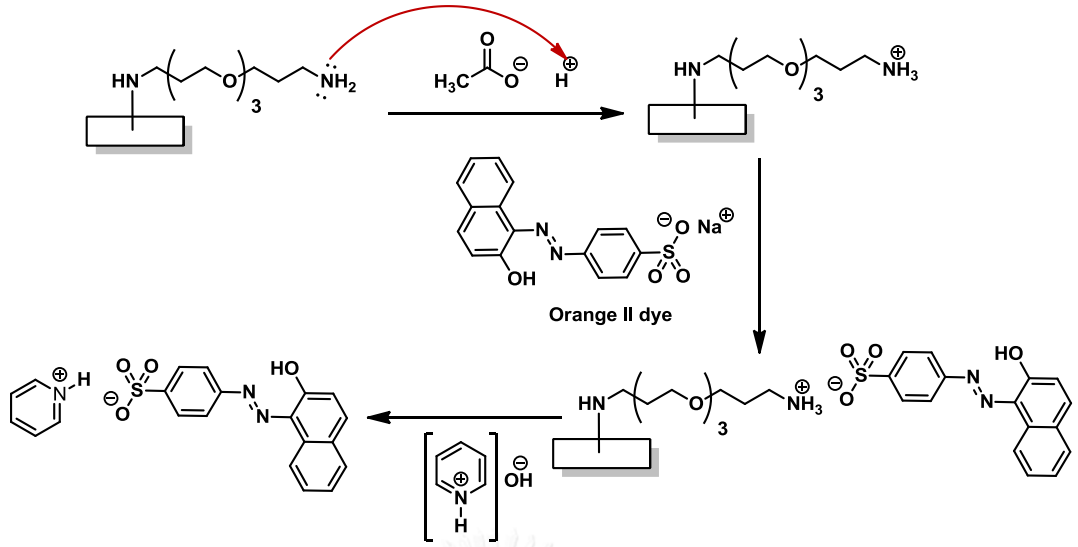

Figure 3.9 The schematic representation of quantification by orange II method.

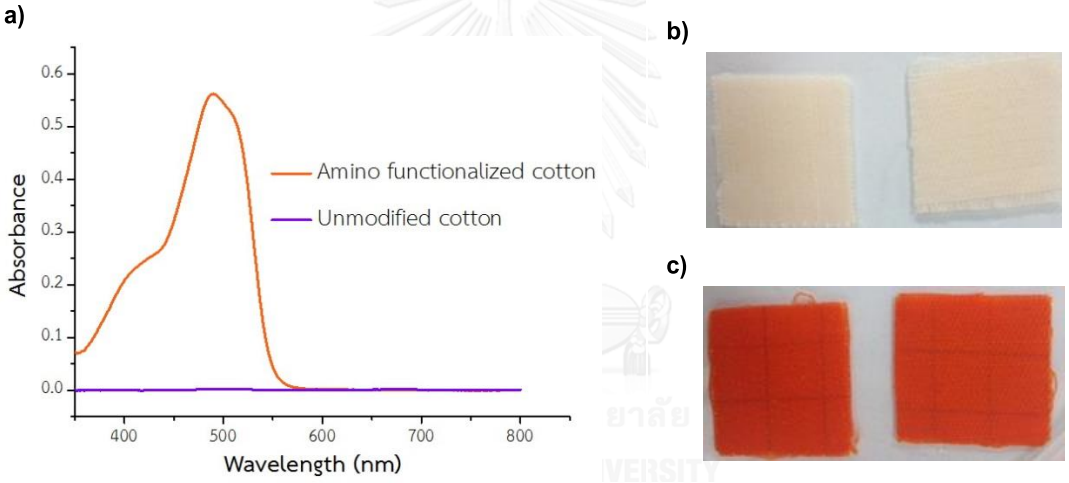

Figure 10 a) Absorption spectra of the CI Acid Orange 7 extracted from amino-functionalized cotton and unmodified cotton. Photo of b) unmodified and c) amino-functionalized cottons after straining with dye.

The absorption spectra of the 25% aqueous pyridine solution containing CI Acid Orange 7 extracted from a dyed amino-functionalized cotton fabric and unmodified cotton are shown in **Figure 10** and dye density was found to be 0.672 μmol/cm^2 for amino functionalized cotton and 0.001 μmol/cm^2 for unmodified cotton.

3.2.3.2 Determination of the peptide loaded on cotton.

Dibenzofulvene piperidine adduct, which was formed in base deprotection step can absorb UV light. This allows for the determination of the amount of peptides at 296 nm. For the determination of the peptides loading, a calibration curve for the deprotection had to be generated by deprotection of Fmoc group from Fmoc-glycine with the solution of 20% piperidine and 2% DBU (**Figure 3.11**). Using a created calibration curve, the loading was then determined (**Table 3.1**).

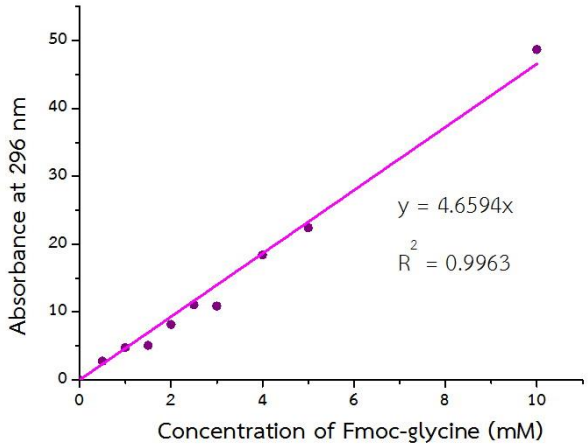

Figure 3.11 Calibration curve for the determination of peptides loading measured by UV/Vis spectroscopy at 296 nm.

Samples	Amount of peptide (μmol/cm^2)	
	with spacer	without spacer
5mer	0.814	0.829
9mer	0.647	0.259
D-9mer	0.649	0.265

Table 3.1 Data of the amount of peptide loaded on the cotton.

3.2.3.3 Scanning Electron Microscopy (SEM) analysis

To investigate the morphology of untreated and peptide-modified cotton surfaces, SEM characterization was performed. **Figure 3.12** shows SEM images with various magnifications of untreated cotton, **5mer**, **5mer.C16**, **L-9mer** with and without a spacer. The results of SEM analysis revealed that the surface was not damaged after the chemical modifications.

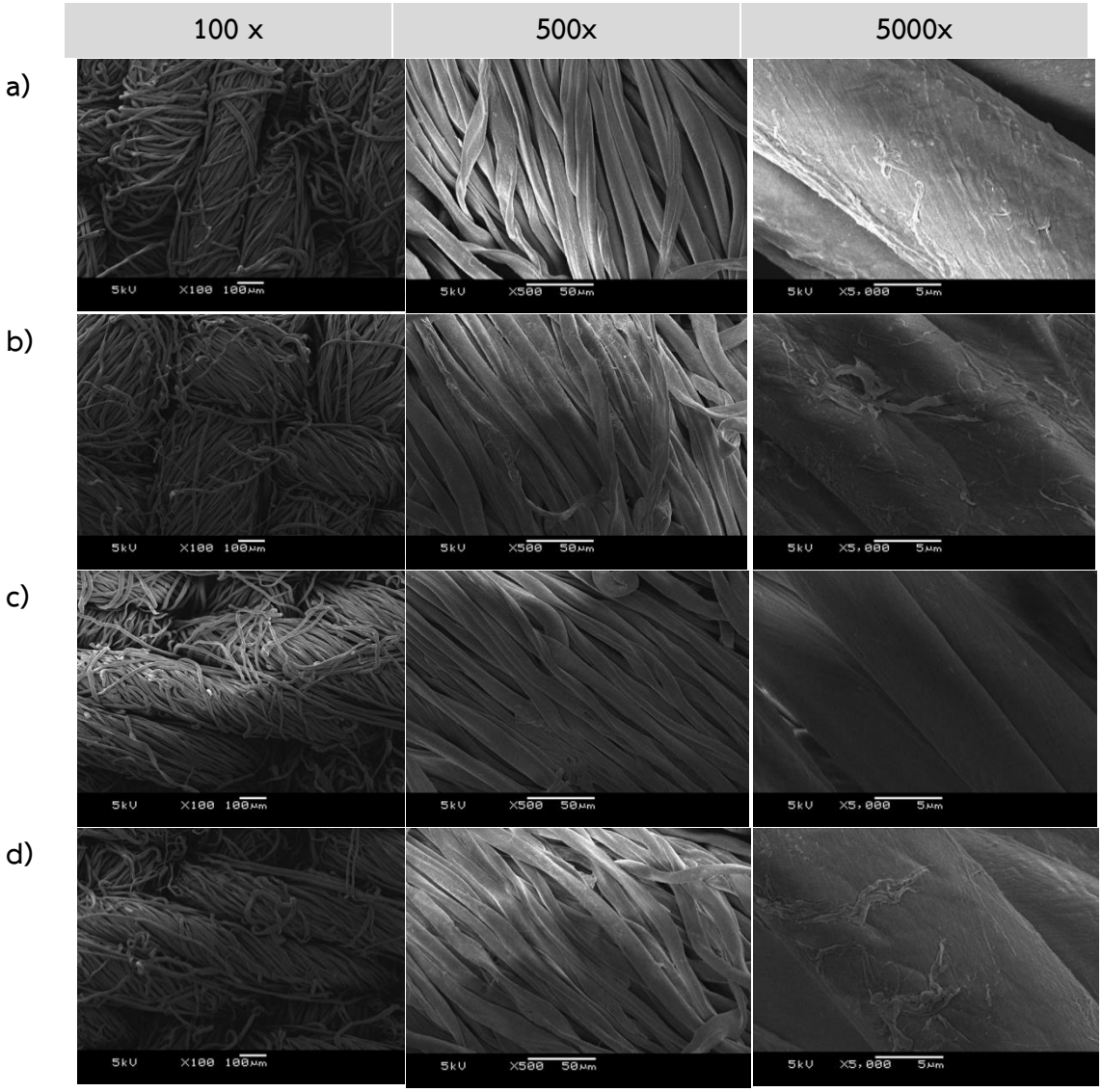

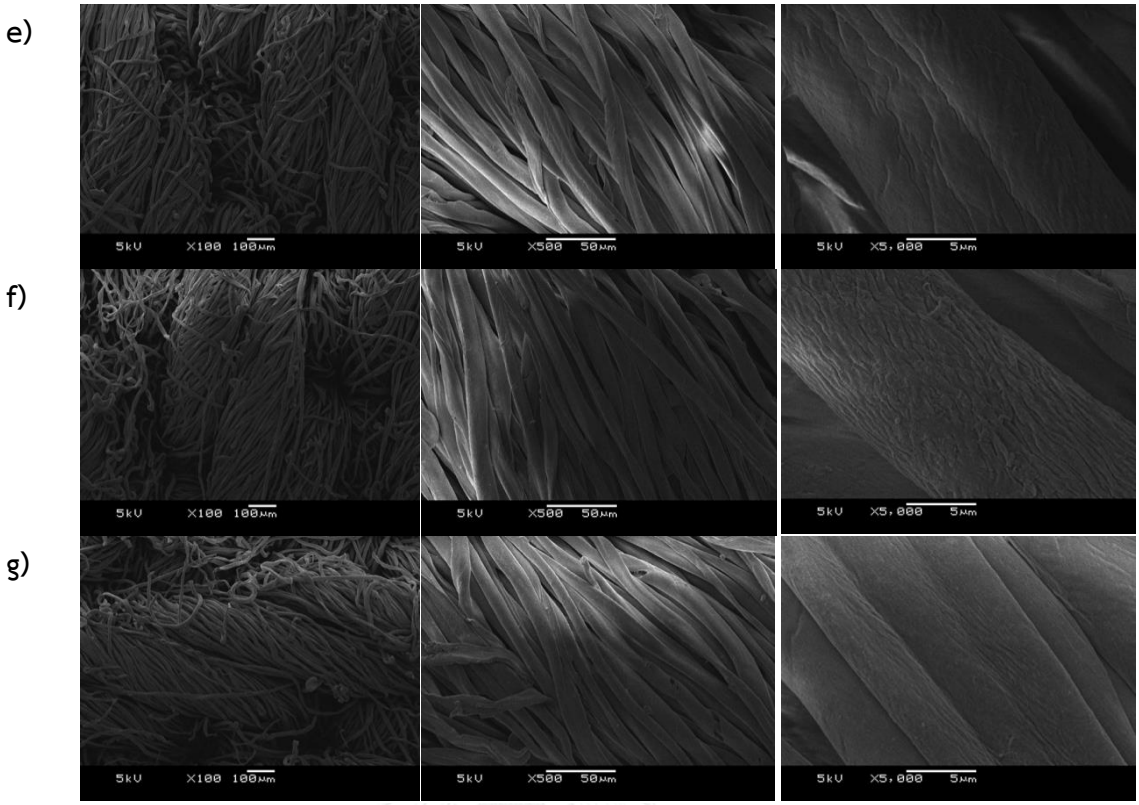

Figure 3.12 SEM images of a) untreated cotton b) **5mer.SP** c) **5mer.C16.SP** d) **9mer.SP** e) **5mer** f) **5mer.C16** and g) **9mer**.

3.2.3.4 MALDI-TOF Mass spectrometry

The peptides that were synthesized on cotton fabric via Rink amide linker can be detached by treatment with TFA-Scavenger. The resulting solutions can be analyzed by MALDI-TOF MS (Microflex, Bruker Daltonics), with α-hydroxy-cinnamic acid as a matrix. The mass spectra of crude peptide were shown in **Table 3.2** (**5mer** : m/z: 656.208, calcd $[M+H]^+$: 656.805, **5mer.C4** : m/z: 726.565, calcd $[M+H]^+$: 726.900, **5mer.C6** : m/z: 754.440, calcd $[M+H]^+$: 754.950, **5mer.C10** : m/z: 810.447, calcd $[M+H]^+$: 811.050, **5mer.C12** : m/z: 838.391, calcd $[M+H]^+$: 839.110, **5mer.C16** : m/z: 894.905, calcd $[M+H]^+$: 895.210, **5mer.C18** : m/z: 922.209, calcd $[M+H]^+$: 923.270, **9mer** : m/z: 1202.247, calcd $[M+H]^+$: 1202.488)

Table 3.2 MALDI-TOF Mass spectra of peptides and lipopeptides cleaved from cotton surfaces.

Samples	Mass spectra
5mer $[M+H]^+$: 656.805	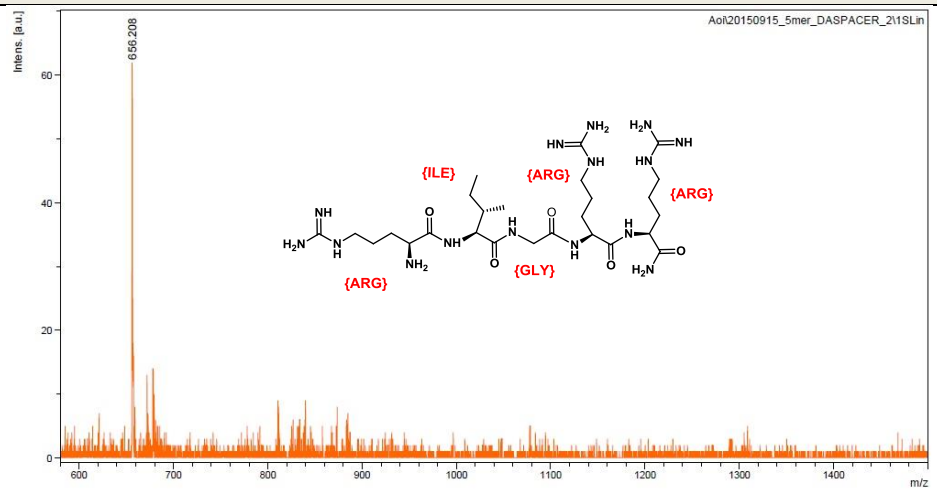
5mer.C4 $[M+H]^+$: 726.900	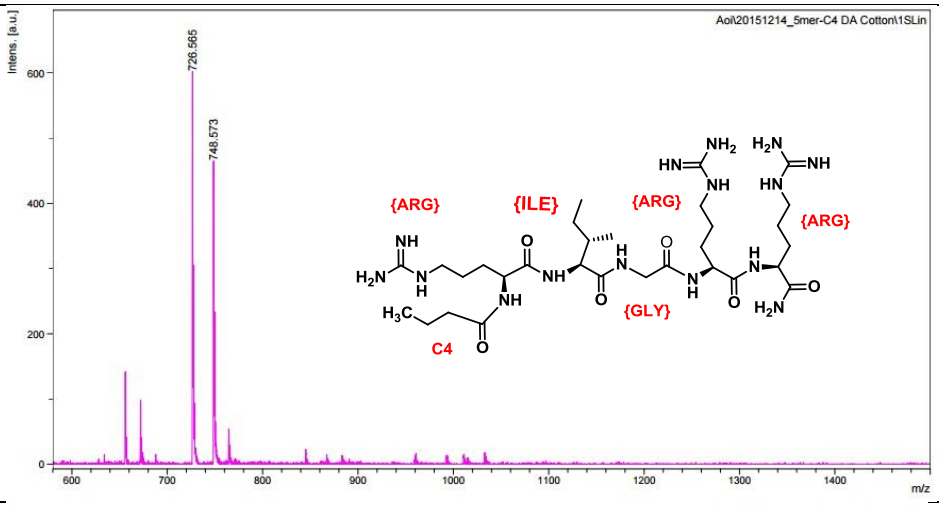
5mer.C6 $[M+H]^+$: 754.950	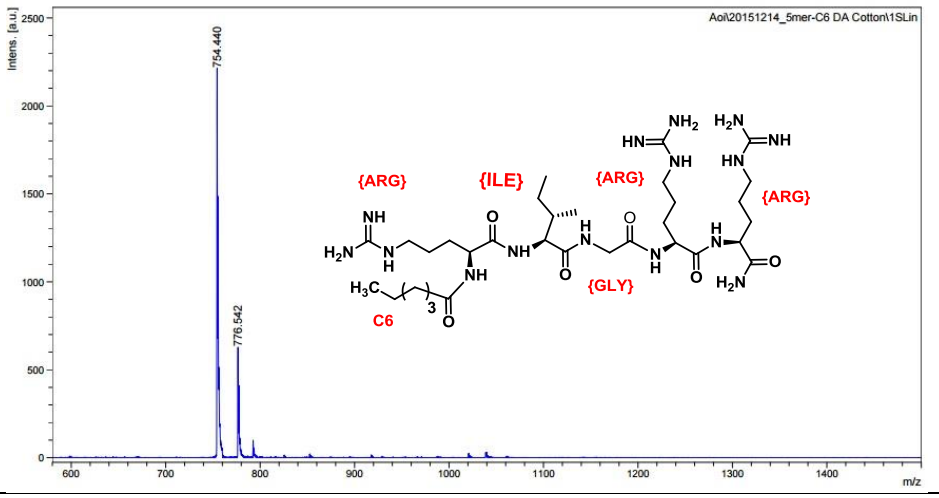

5mer.C10 $[M+H]^+$: 811.050	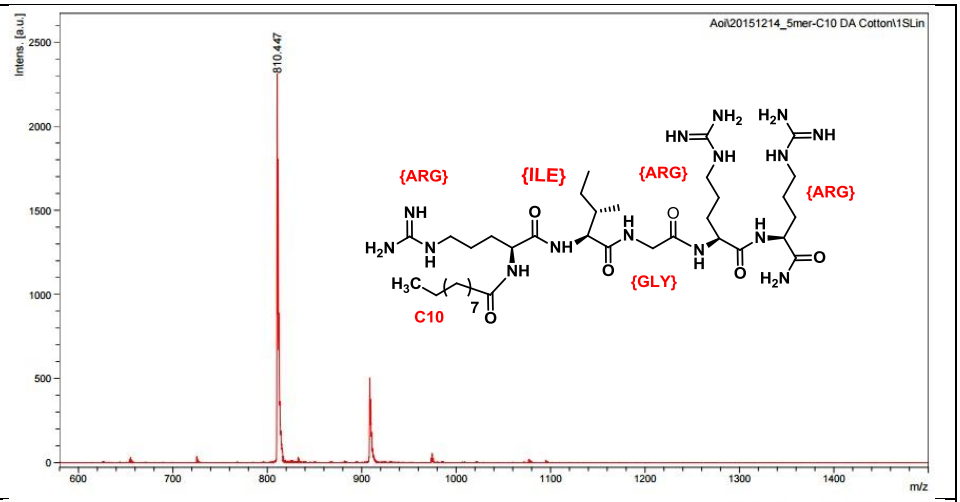
5mer.C12 $[M+H]^+$: 839.110	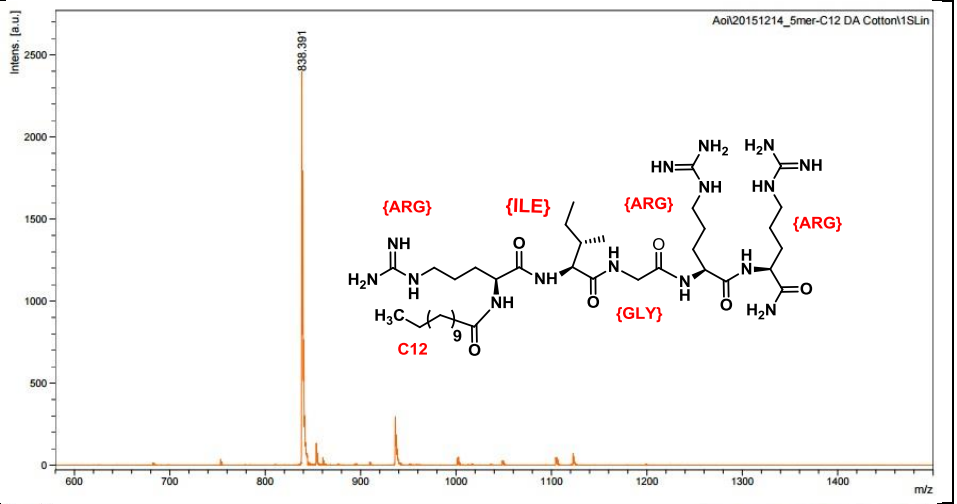
5mer.C16 $[M+H]^+$: 895.210	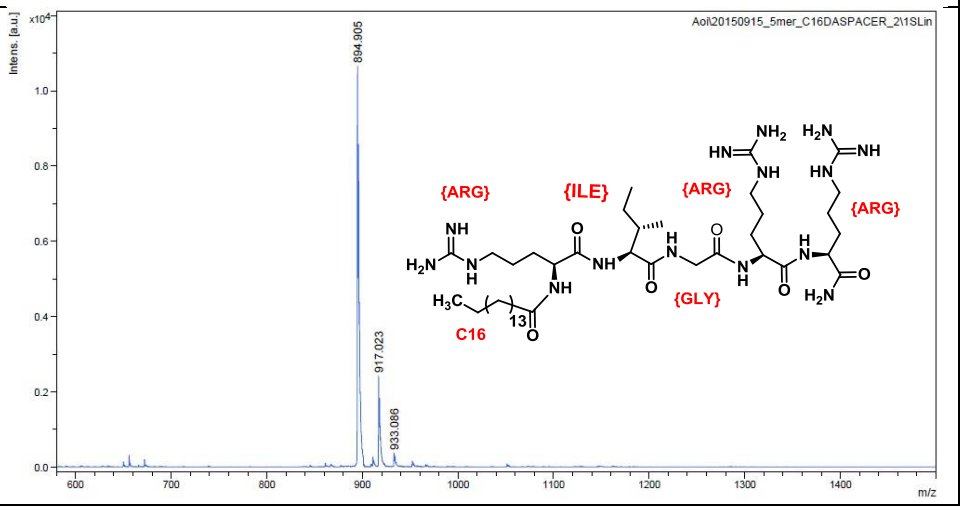

5mer.C18 $[M+H]^+$: 923.270	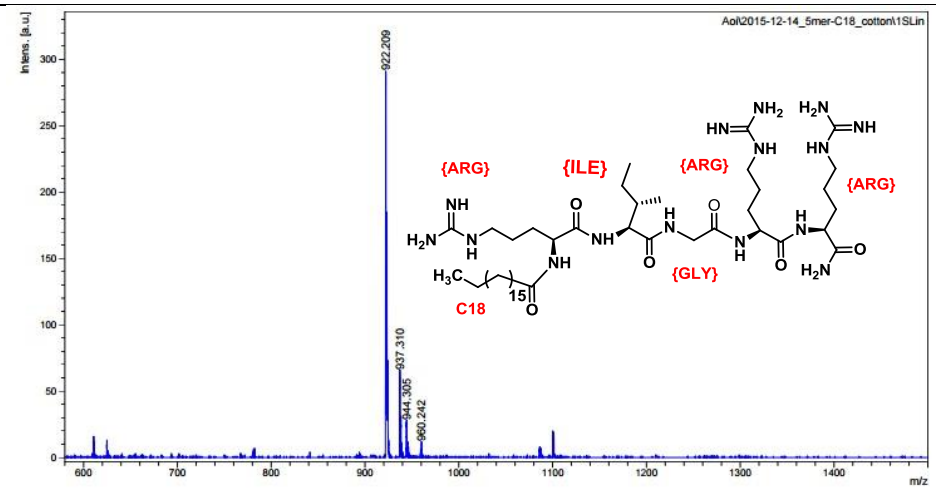
9mer $[M+H]^+$: 1202.488	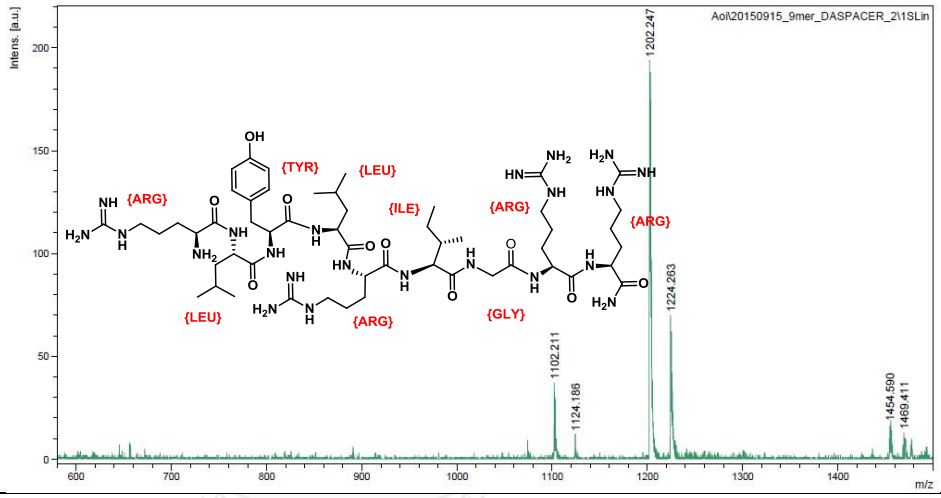

3.3 Antibacterial activity of peptides and lipopeptides-immobilized surfaces

3.3.1 Bacterial culture

The measurement of bacterial growth can be done by determining the turbidity of bacterial cultures at 620 nm. Growth curves of *P. aeruginosa*, *E. coli* and *S. aureus* are shown in **Figure 3.13**. We observe that the mid -exponential points are 0.6, 0.7 and 0.7 in *P. aeruginosa*, *E. coli* and *S. aureus*, respectively. During this phase, the bacterial cells are growing and dividing at the maximum rate. All bacteria in the suspension are considered to be the same physiological properties [3].

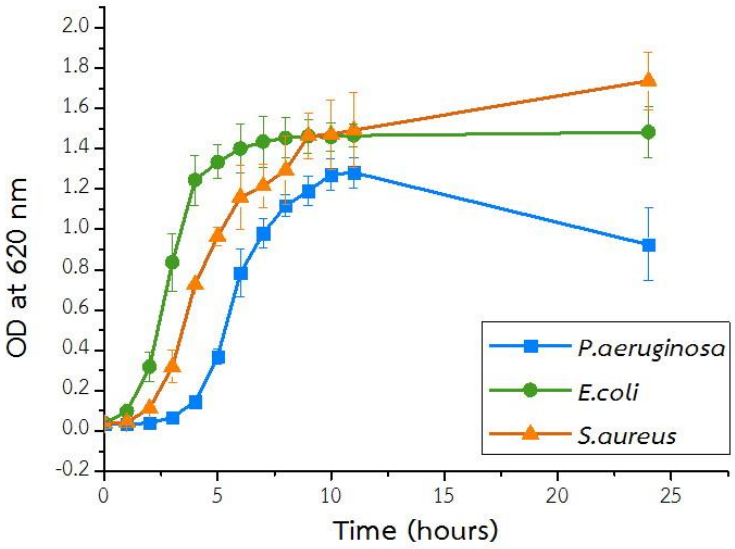

Figure 3.13 Comparison between growth curves of *P. aeruginosa*, *E. coli* and *S. aureus* at 37°C

3.3.2 The antibacterial assays

The antibacterial activities of peptide-immobilized cotton fabrics were quantitatively determined by colony counting method (Japanese Industrial Standard, JIS L 1902) against Gram-positive bacterium (*S. aureus*-ATTC 6538P), and Gram-negative bacteria (*E. coli*-ATCC 8739, and *P. aeruginosa*-ATTC 9027). In the case of *S.aureus*, lower log colony forming unit (CFU/mL) values indicated higher

antibacterial activity. The antibacterial activities of samples was tested and shown in **Figure 3.14**. The result of counting test showed the highest log reduction of surviving bacteria in the case of **5mer.C6.SP**. Interestingly, almost all samples with the spacer had higher antibacterial activities than those without the spacer because the spacer may increase the flexibility of peptides resulting in effective bacterial inhibition. The lipopeptides significantly increased the potency, up to the acyl chain with twelve carbon atoms and ten carbon atoms (with and without diamine spacers, respectively).

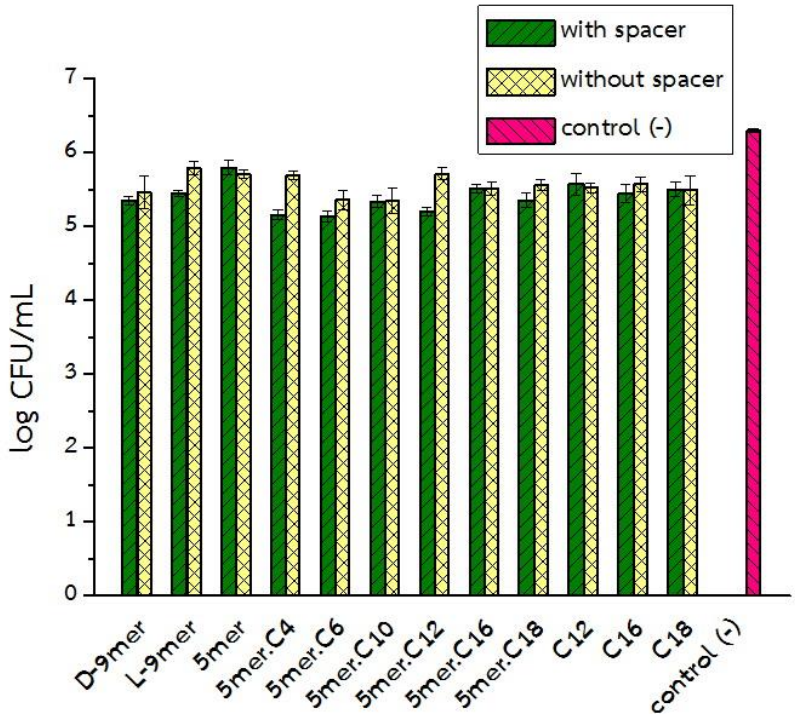

Figure 3.14 Antibacterial activities of modified cotton fabrics in *S. aureus.*

In the case of *E. coli* (ATCC 8739) and *P. aeruginosa* (ATCC 9027) , almost all peptides showed complete killing, However, all of the cotton fabrics with directly coupled fatty acids showed lower antibacterial activities in these strains (**Figure 3.15, Figure 3.16**). The higher activities of samples in Gram-negative bacteria were believed to be due to the difference in cell wall structures. Gram-positive bacteria have a thick peptidoglycan layer (20-80 nm), while the peptidoglycan layer

in Gram-negative bacteria is thin (7-8 nm). In addition, lipopolysaccharide layer on the outer membrane of Gram-negative bacteria is not as rigid as peptidoglycan.

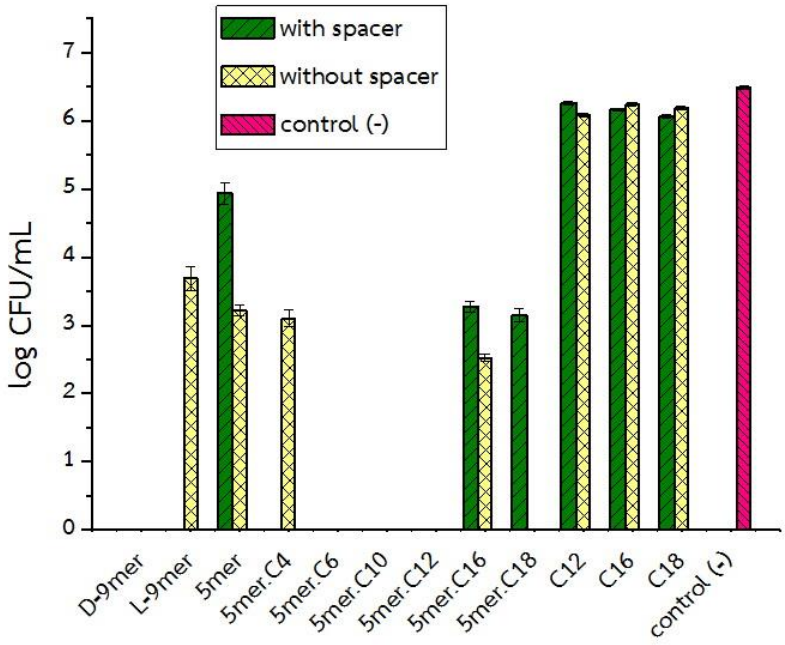

Figure 3.15 Antibacterial activities of modified cotton fabrics in *E. coli.*

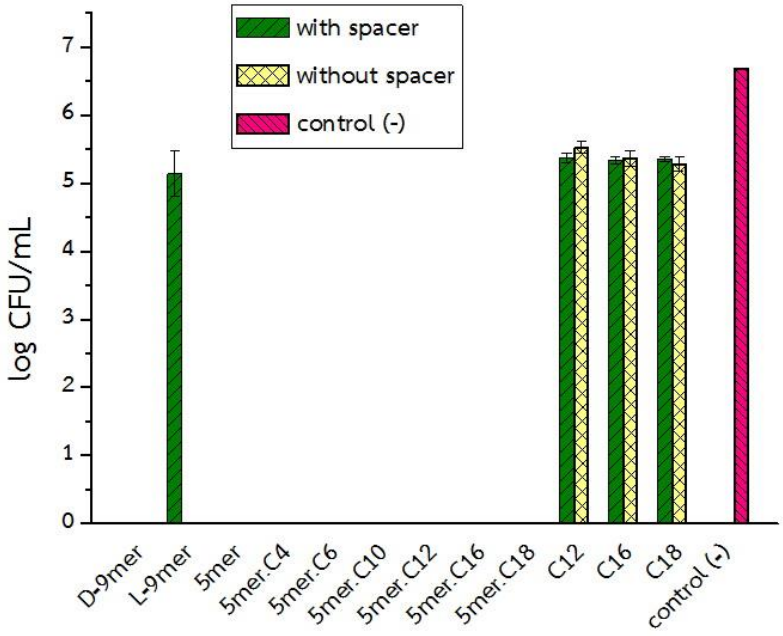

Figure 3.16 Antibacterial activities of modified cotton fabrics in *P. aeruginosa.*

The mechanism of bactericidal properties of lipopeptide-immobilized cotton fabrics is still not resolved. However, based on previous studies, it was proposed that the disruption of bacterial cell membrane is likely the major factor. The mode of action is based on electrostatic interaction of the positively charged arginine and the negatively charged lipopolysaccharide of Gram-negative bacteria and lipoteichoic acid of Gram-positive bacterial membrane (**Figure 3.17a**). The hydrophobic moieties of lipopeptides were inserted into lipid bilayer structure of bacterial membranes [25] (**Figure 3.17b**) or the positively charged arginines pull anionic phospholipids out of the bacterial membrane [26] (**Figure 3.17c**), thereby causing membrane permeabilization by pore formation, leading to cell lysis and death (**Figure 3.17d**).

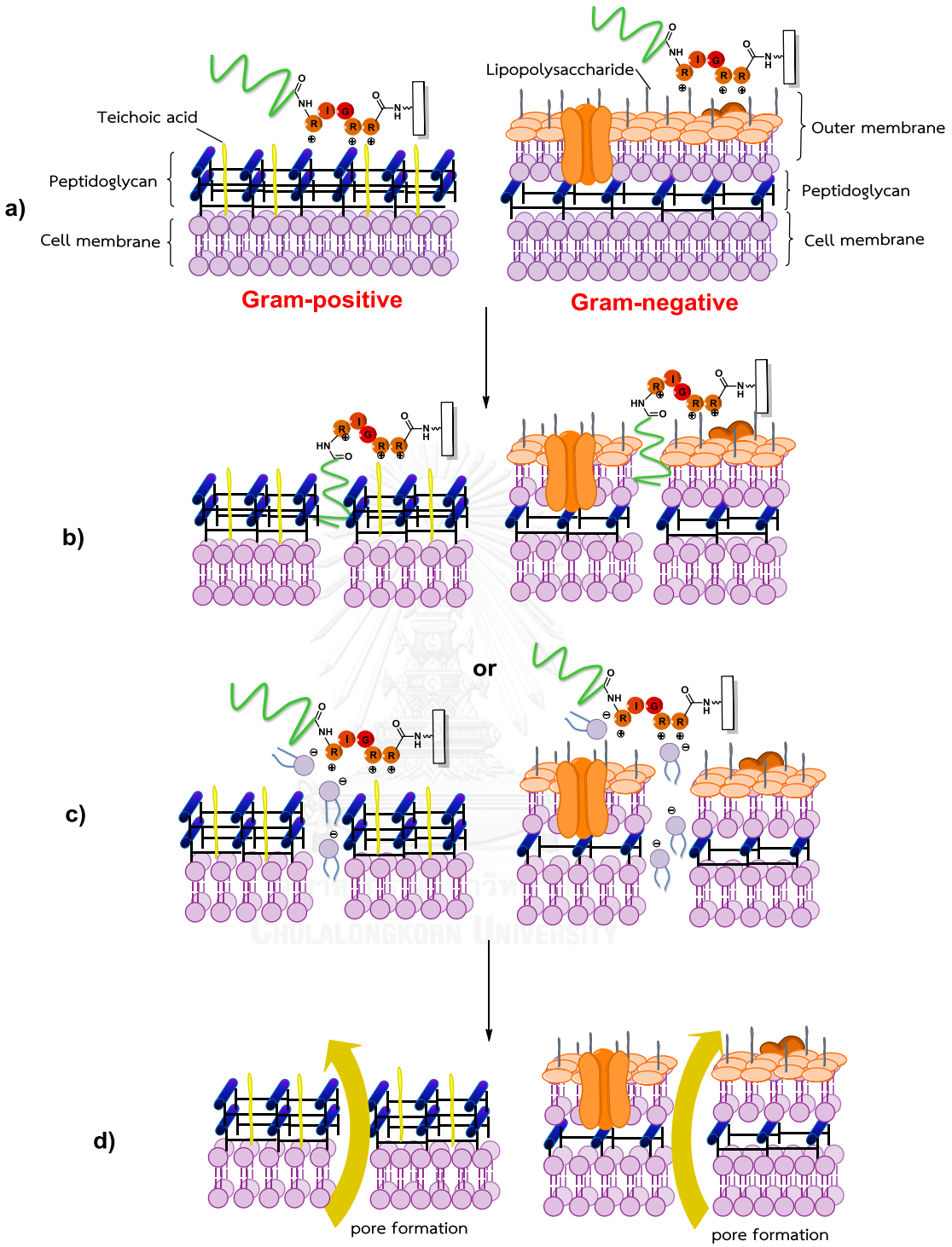

Figure 3.17 Proposed mechanism of lipopeptides-immobilized cotton surface.

3.4 Biocompatibility assay

The biocompatibility of peptide-immobilized cotton fabrics was quantitatively determined by cell viability assay. The L929 mouse fibroblast cell line was analyzed after direct contact with **5mer.C4.SP**, **5mer.C12.SP**, and **5mer.C16** for different time periods (24, 48, 72 h) and the number of cells adhered to the surface of the samples was determined by quantification of the MTT metabolic activity. The resulting color change of a yellow colored tetrazolium salt to purple colored formazan is directly related to cell metabolic activity. Cell viability over 70% meant that all of the samples were not cytotoxic to fibroblast cells (**Figure 3.18**).

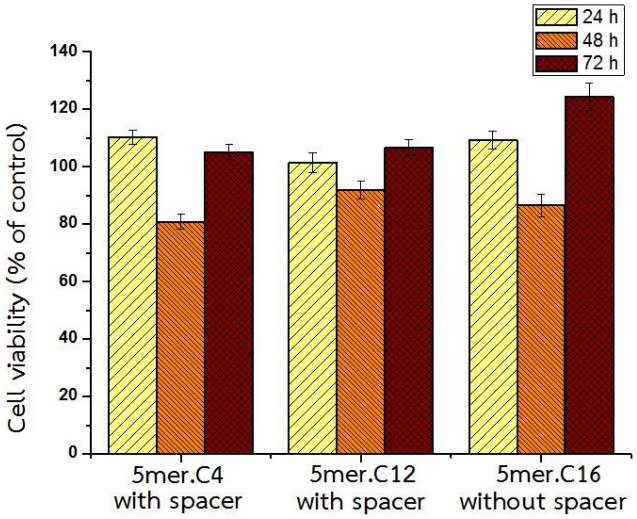

Figure 3.18 Biocompatibility of modified cotton fabrics with L929 mouse fibroblast.

CHAPTER IV

CONCLUSIONS

In this research, a novel class of peptides was synthesized and immobilized on cotton fabrics. This consisted of a 5-mer peptide (RIGRR), which was further conjugated with different lengths (C4-C18) of linear fatty acids through standard carbodiimide coupling and Fmoc protection strategy. Additionally, the effect of an amino molecular spacer inserted between the cellulose surface and the first amino acid was also studied.

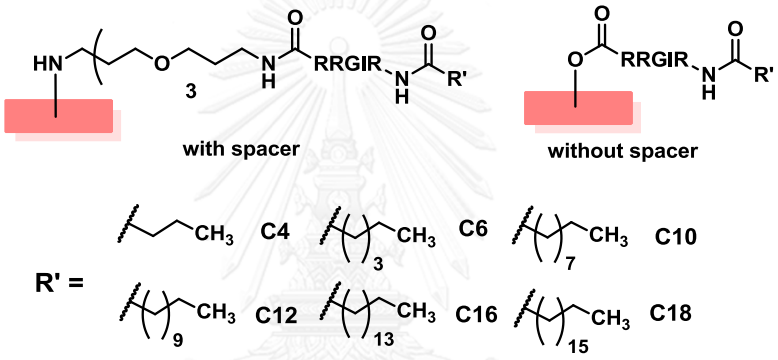

Figure 4.1 The lipopeptide-immobilized cotton surfaces.

The modified cotton surfaces were subsequently tested for bacterial growth inhibition against two bacterial types: a Gram-positive bacterium (*Staphylococcus aureus*-ATTC 6538P), and Gram-negative bacteria (*Escherichia coli*-ATCC 8739, and *Pseudomonas aeruginosa*-ATTC 9027) using the Japanese Industrial Standard (JIS) L 1902. The results showed more activity on Gram-negative than Gram-positive bacteria possibly due to their easier permeation into the Gram-negative bacterial membrane. Most samples with the spacer had higher antibacterial activity than those without the spacer. Furthermore, the measurement of cell viability of the modified peptide to L929 mouse fibroblast cell demonstrated that the surfaces were non-toxic to human cells.

REFERENCES

1. Rodrigues, L. R., Inhibition of Bacterial Adhesion on Medical Devices. In *Bacterial Adhesion: Chemistry, Biology and Physics*, Linke, D.; Goldman, A., Eds. Springer Netherlands: Dordrecht, 2011; pp 351-367.

2. Epand, R. M.; Walker, C.; Epand, R. F.; Magarvey, N. A., Molecular mechanisms of membrane targeting antibiotics. *Biochimica et Biophysica Acta (BBA) - Biomembranes* **2016,** *1858* (5), 980-987.

3. Prescott, L.; Harley, J. P.; Klein, D. A., *Microbiology*. The McGraw-Hill Companies: 1999.

4. Otto, M., Staphylococcus aureus toxins. *Current Opinion in Microbiology* **2014,** *17*, 32-37.

5. Driscoll, J. A.; Brody, S. L.; Kollef, M. H., The epidemiology, pathogenesis and treatment of Pseudomonas aeruginosa infections. *Drugs* **2007,** *67* (3), 351-68.

6. Siedenbiedel, F.; Tiller, J. C., Antimicrobial Polymers in Solution and on Surfaces: Overview and Functional Principles. *Polymers* **2012,** *4* (1), 46.

7. Yu, Q.; Wu, Z.; Chen, H., Dual-function antibacterial surfaces for biomedical applications. *Acta Biomaterialia* **2015,** *16*, 1-13.

8. Abel, T.; Cohen, J. I.; Engel, R.; Filshtinskaya, M.; Melkonian, A.; Melkonian, K., Preparation and investigation of antibacterial carbohydrate-based surfaces. *Carbohydrate Research* **2002,** *337* (24), 2495-2499.

9. Song, J.; Kang, H.; Lee, C.; Hwang, S. H.; Jang, J., Aqueous Synthesis of Silver Nanoparticle Embedded Cationic Polymer Nanofibers and Their Antibacterial Activity. *ACS Applied Materials & Interfaces* **2012,** *4* (1), 460-465.

10. Knetsch, M. L. W.; Koole, L. H., New Strategies in the Development of Antimicrobial Coatings: The Example of Increasing Usage of Silver and Silver Nanoparticles. *Polymers* **2011,** *3* (1), 340.

11. Ekblad, T.; Bergström, G.; Ederth, T.; Conlan, S. L.; Mutton, R.; Clare, A. S.; Wang, S.; Liu, Y.; Zhao, Q.; D'Souza, F.; Donnelly, G. T.; Willemsen, P. R.; Pettitt, M. E.; Callow, M. E.; Callow, J. A.; Liedberg, B., Poly(ethylene glycol)-Containing Hydrogel

Surfaces for Antifouling Applications in Marine and Freshwater Environments. *Biomacromolecules* **2008,** *9* (10), 2775-2783.

12. Zhang, X.; Wang, L.; Levanen, E., Superhydrophobic surfaces for the reduction of bacterial adhesion. *RSC Advances* **2013,** *3* (30), 12003-12020.

13. Wang, G.; Mishra, B.; Lau, K.; Lushnikova, T.; Golla, R.; Wang, X., Antimicrobial Peptides in 2014. *Pharmaceuticals* **2015,** *8* (1), 123-150.

14. Shai, Y., Mechanism of the binding, insertion and destabilization of phospholipid bilayer membranes by **α**-helical antimicrobial and cell non-selective membrane-lytic peptides. *Biochimica et Biophysica Acta (BBA) - Biomembranes* **1999,** *1462* (1–2), 55-70.

15. Zhang, M.; Zhao, J.; Zheng, J., Molecular understanding of a potential functional link between antimicrobial and amyloid peptides. *Soft Matter* **2014,** *10* (38), 7425-7451.

16. Silva, P. M.; Gonçalves, S.; Santos, N. C., Defensins: antifungal lessons from eukaryotes. *Frontiers in Microbiology* **2014,** *5*.

17. Willcox, M. D.; Hume, E. B.; Aliwarga, Y.; Kumar, N.; Cole, N., A novel cationic-peptide coating for the prevention of microbial colonization on contact lenses. *Journal of applied microbiology* **2008,** *105* (6), 1817-25.

18. Lim, K.; Chua, R. R. Y.; Saravanan, R.; Basu, A.; Mishra, B.; Tambyah, P. A.; Ho, B.; Leong, S. S. J., Immobilization Studies of an Engineered Arginine–Tryptophan-Rich Peptide on a Silicone Surface with Antimicrobial and Antibiofilm Activity. *ACS Applied Materials & Interfaces* **2013,** *5* (13), 6412-6422.

19. Etayash, H.; Norman, L.; Thundat, T.; Stiles, M.; Kaur, K., Surface-Conjugated Antimicrobial Peptide Leucocin A Displays High Binding to Pathogenic Gram-Positive Bacteria. *ACS Applied Materials & Interfaces* **2014,** *6* (2), 1131-1138.

20. Hilpert, K.; Elliott, M.; Jenssen, H.; Kindrachuk, J.; Fjell, C. D.; Körner, J.; Winkler, D. F. H.; Weaver, L. L.; Henklein, P.; Ulrich, A. S.; Chiang, S. H. Y.; Farmer, S. W.; Pante, N.; Volkmer, R.; Hancock, R. E. W., Screening and Characterization of Surface-Tethered Cationic Peptides for Antimicrobial Activity. *Chemistry & Biology* **2009,** *16* (1), 58-69.

21. Nakamura, M.; Iwasaki, T.; Tokino, S.; Asaoka, A.; Yamakawa, M.; Ishibashi, J., Development of a Bioactive Fiber with Immobilized Synthetic Peptides Designed from the Active Site of a Beetle Defensin. *Biomacromolecules* **2011,** *12* (5), 1540-1545.

22. Roy, D.; Semsarilar, M.; Guthrie, J. T.; Perrier, S., Cellulose modification by polymer grafting: a review. *Chemical Society Reviews* **2009,** *38* (7), 2046-2064.

23. Al-Warhi, T. I.; Al-Hazimi, H. M. A.; El-Faham, A., Recent development in peptide coupling reagents. *Journal of Saudi Chemical Society* **2012,** *16* (2), 97-116.

24. Noel, S.; Liberelle, B.; Robitaille, L.; De Crescenzo, G., Quantification of Primary Amine Groups Available for Subsequent Biofunctionalization of Polymer Surfaces. *Bioconjugate Chemistry* **2011,** *22* (8), 1690-1699.

25. Sato, H.; Feix, J. B., Peptide–membrane interactions and mechanisms of membrane destruction by amphipathic α-helical antimicrobial peptides. *Biochimica et Biophysica Acta (BBA) - Biomembranes* **2006,** *1758* (9), 1245-1256.

26. Yatvin, J.; Gao, J.; Locklin, J., Durable defense: robust and varied attachment of non-leaching poly"-onium" bactericidal coatings to reactive and inert surfaces. *Chemical Communications* **2014,** *50* (67), 9433-9442.

APPENDIX

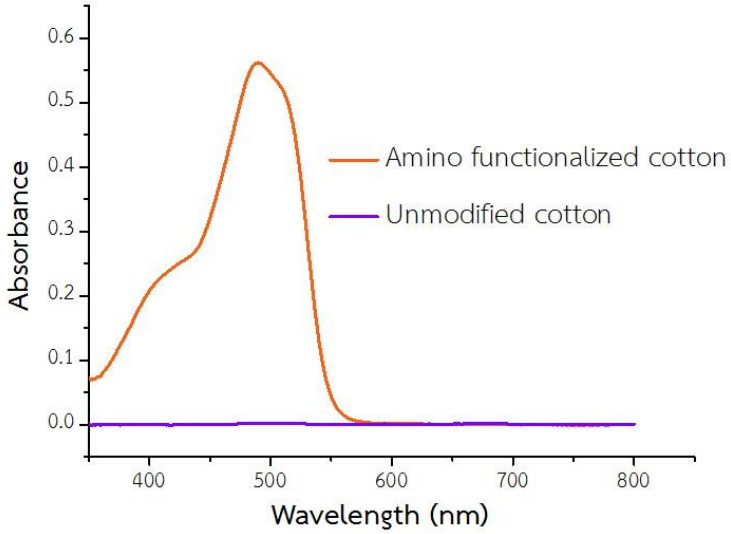

Figure A.1 Absorption spectra of the CI Acid Orange 7 extracted from amino-functionalized cotton and unmodified cotton.

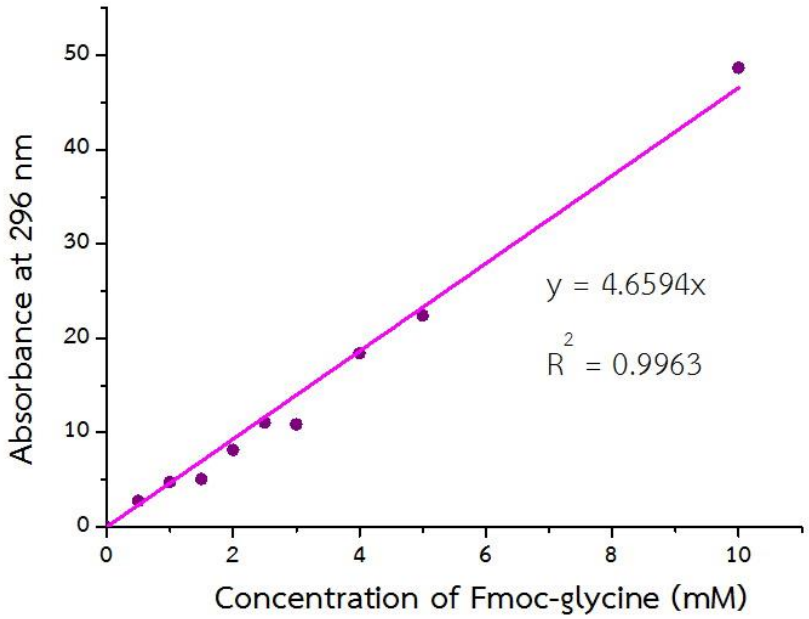

Figure A.2 Calibration curve for the determination of peptides loading measured by UV/Vis spectroscopy at 296 nm.

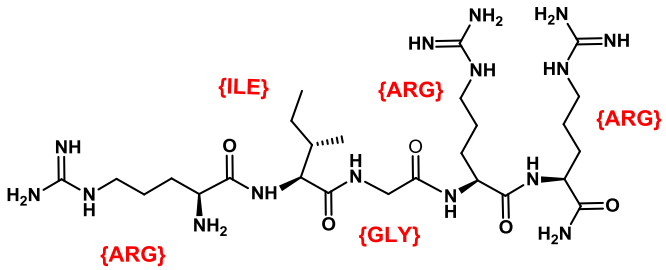

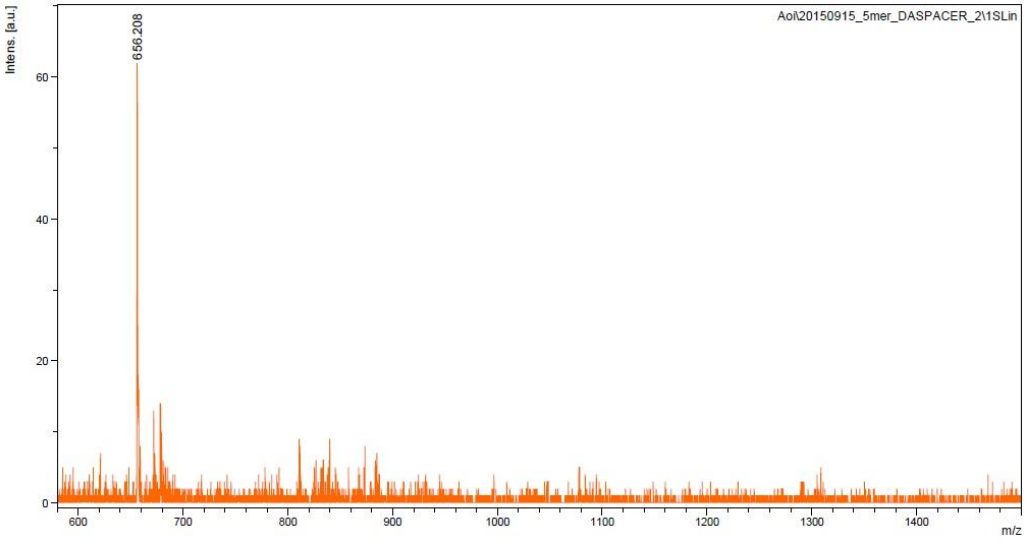

Figure A.3 Structure and MALDI-TOF mass spectrum of **5mer** peptide (**RIGRR**)

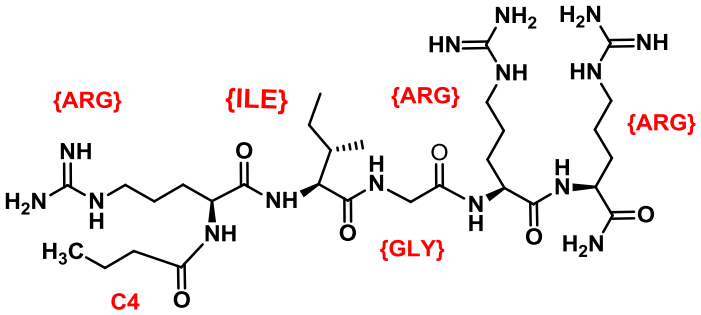

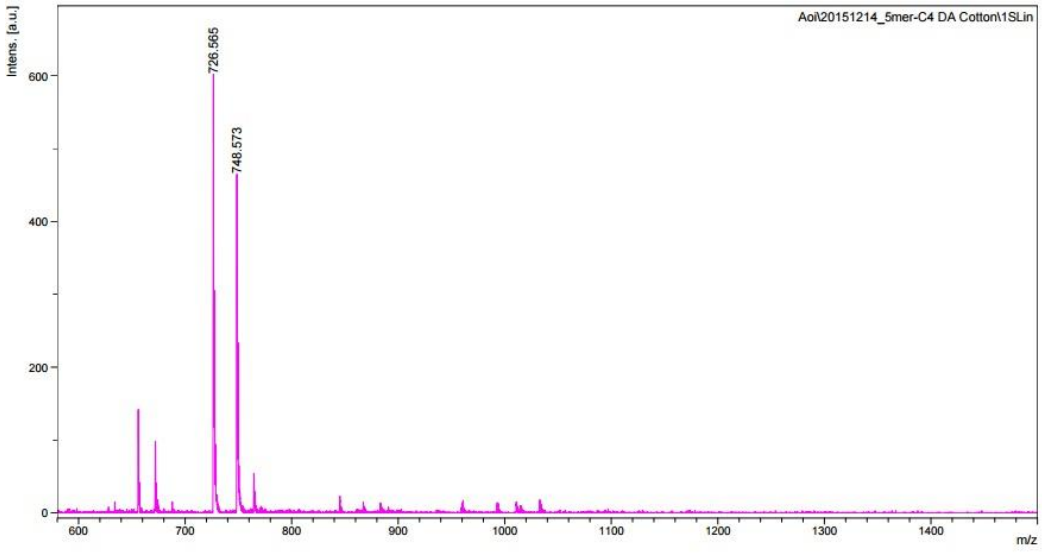

Figure A.4 Structure and MALDI-TOF mass spectrum of **5mer.C4** peptide (**C4-RIGRR**)

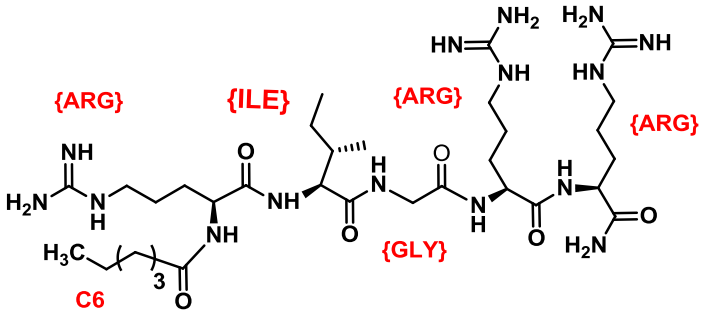

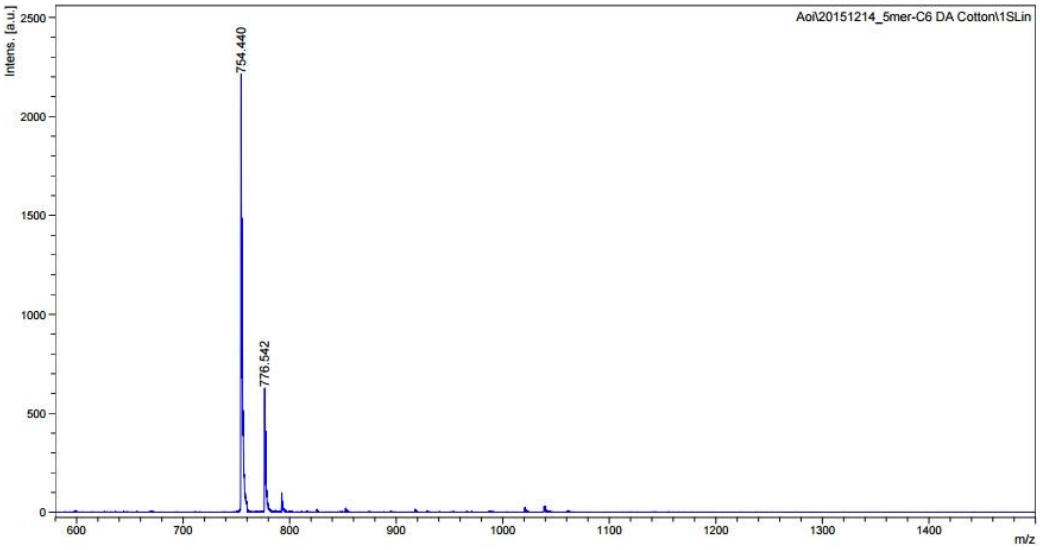

Figure A.5 Structure and MALDI-TOF mass spectrum of **5mer.C6** peptide (**C6-RIGRR**)

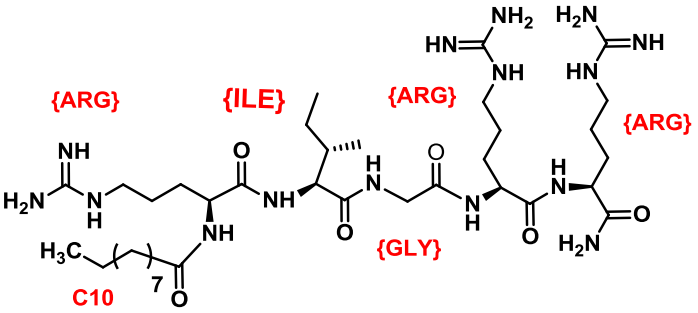

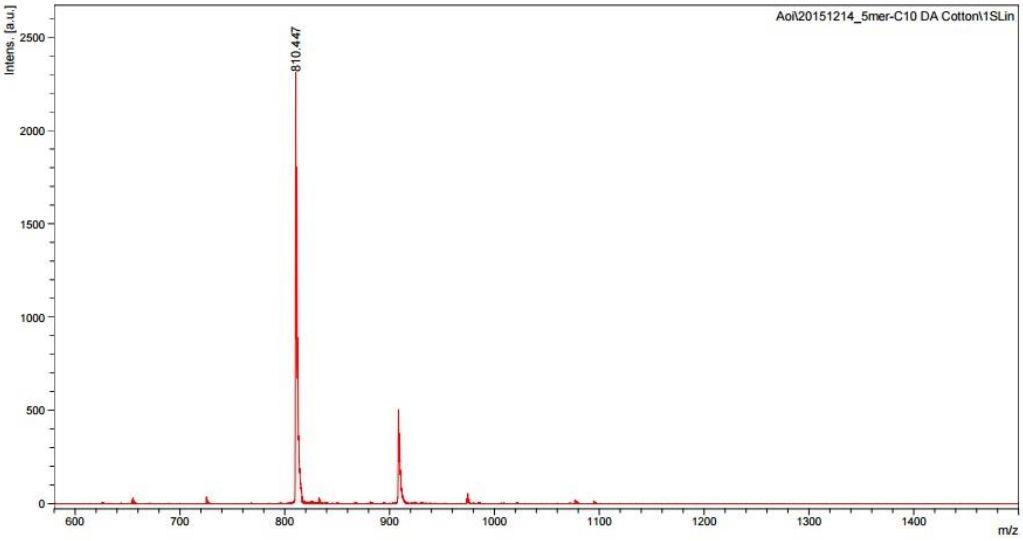

Figure A.6 Structure and MALDI-TOF mass spectrum of **5mer.C10** peptide (**C10-RIGRR**)

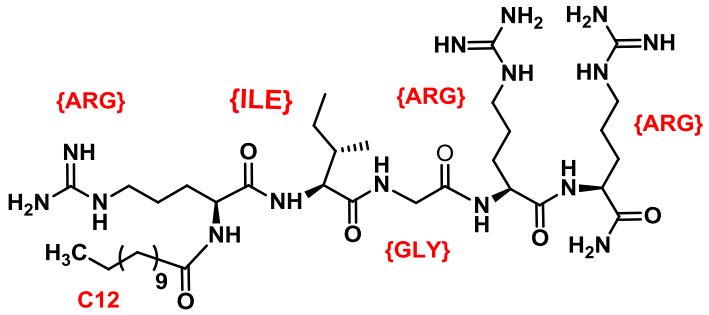

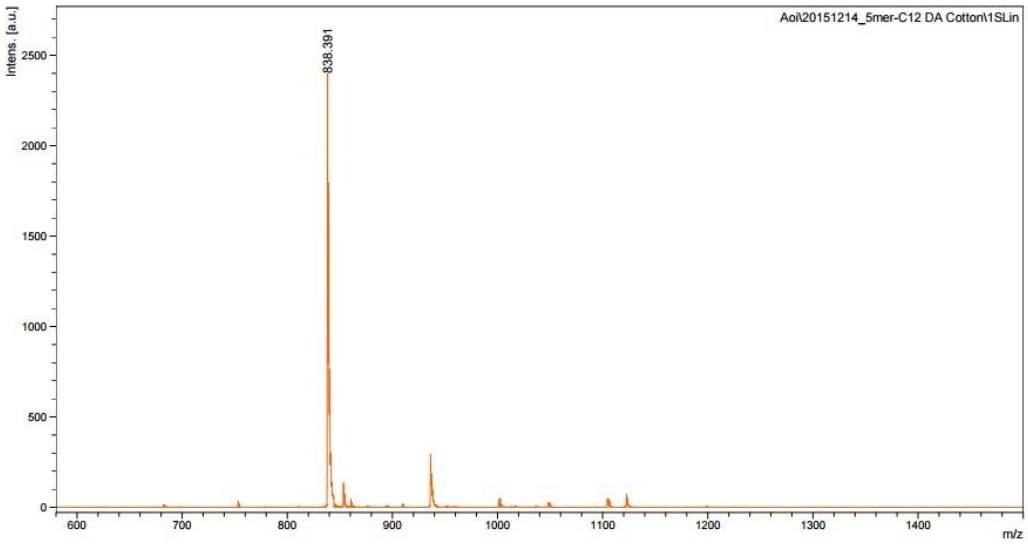

Figure A.7 Structure and MALDI-TOF mass spectrum of **5mer.C12** peptide (**C12-RIGRR**)

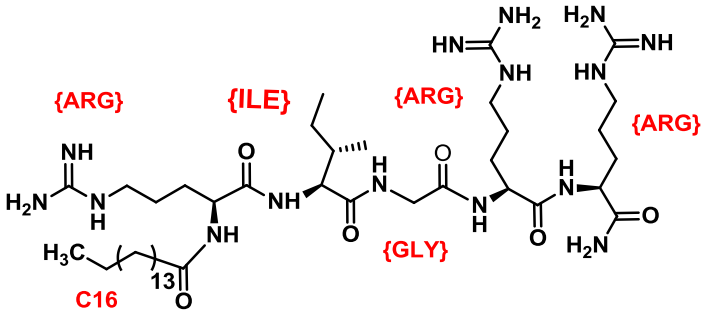

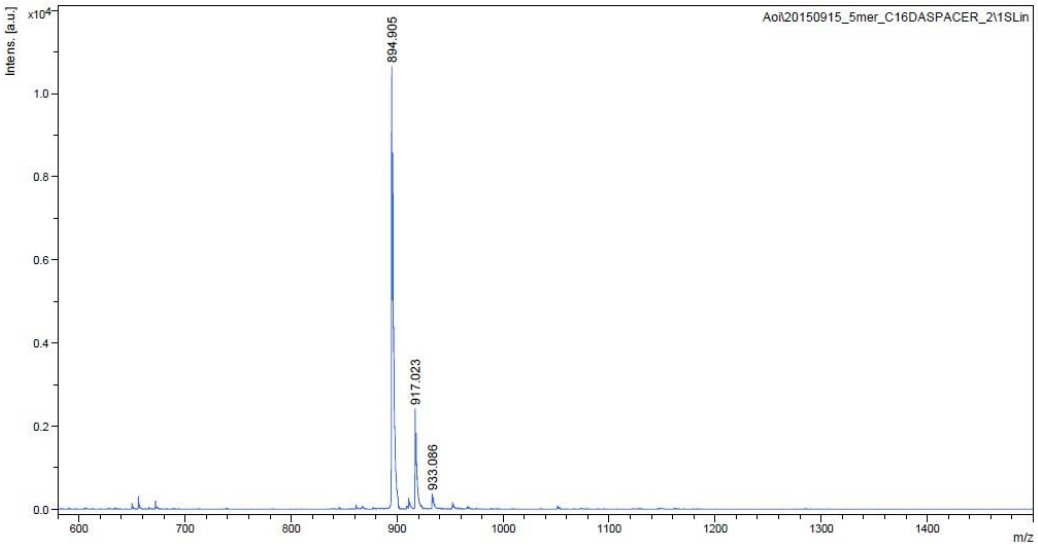

Figure A.8 Structure and MALDI-TOF mass spectrum of **5mer.C16** peptide (**C16-RIGRR**)

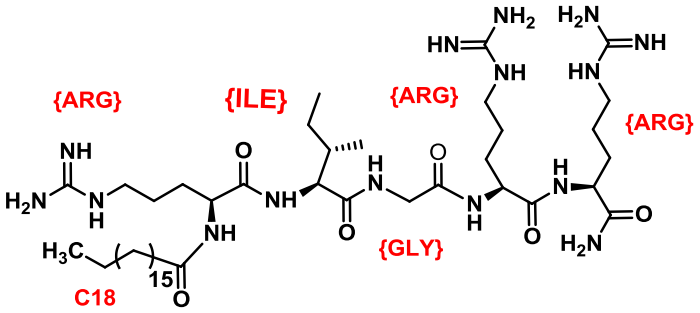

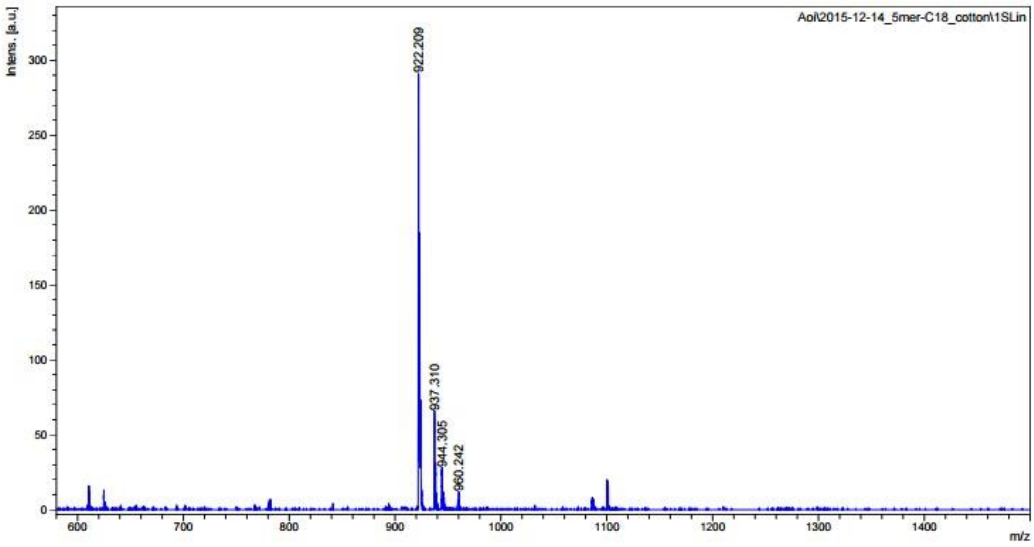

Figure A.9 Structure and MALDI-TOF mass spectrum of **5mer.C18** peptide (**C18-RIGRR**)

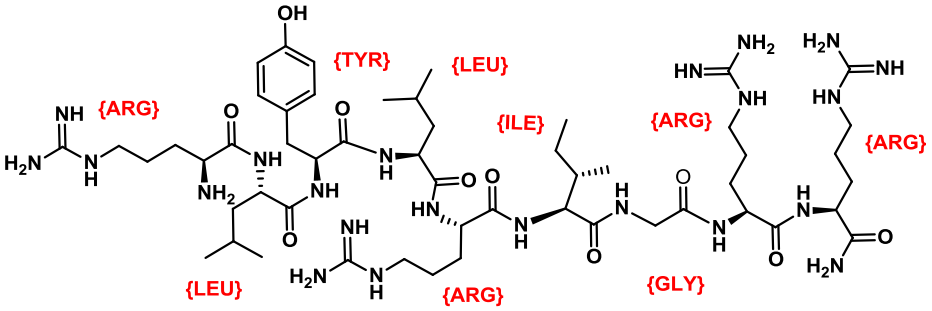

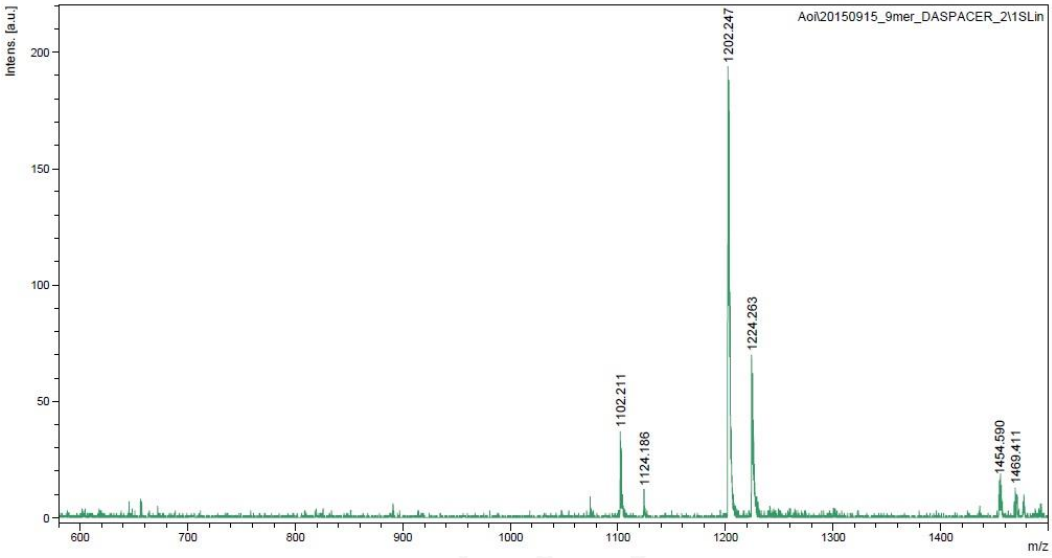

Figure A.10 Structure and MALDI-TOF mass spectrum of **9mer** peptide (**RLYLRIGRR**)

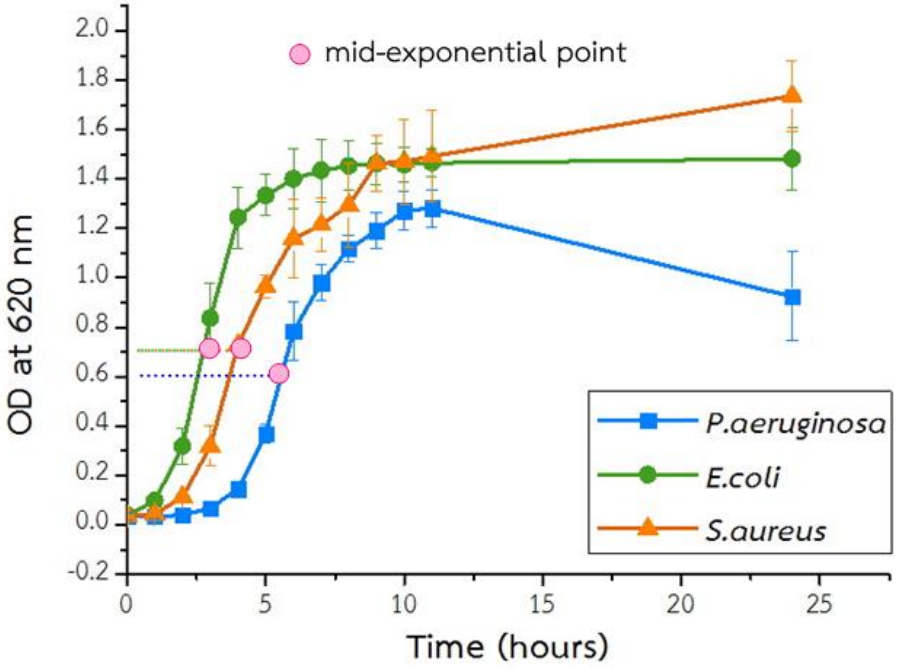

Figure A.11 Comparison between growth curves of *S. aureus*-ATTC 6538P, *E. coli*-ATCC 8739, and *P. aeruginosa*-ATTC 9027 at 37°C

VITA

Miss Apiradee Opitakorn was born on April 8th, 1990 in Phatthalung, Thailand. She began her study in Phatthalung School. Then, she graduated Bachelor's Degree of Science, major in Chemistry from Faculty of Science, Srinakharinwirot University in 2012 under the support from Science Achievement Scholarship of Thailand. She began studying organic chemistry her Master's degree at the Department of Chemistry, Faculty of Science, Chulalongkorn University.

Her present address is 18/1 Thanbumrung Road, Tambon Khuha Sawan, Amphoe Mueang Phatthalung, Phatthalung, 93000, e-mail : apiradeeopi@gmail.com